Nitrogen oxides and ozone from B-747 measurements (NOXAR) during POLINAT 2 and SONEX - Overview and case-studies on continental and marine convection

Dominique P. Jeker [1]
Lenny Pfister [2]
Dominik Brunner [3]
Dennis J. Boccippio [4]
Kenneth E. Pickering [5]
Anne M. Thompson [6]
Heini Wernli [1]
Rennie B. Selkirk [2]
Yutaka Kondo [7]
Matoke Koike [7]
Yongjing Zhao [7]
Johannes Staehelin [1 (*)]

(*) to whom correspondence should be addressed

[1] Institute for Atmospheric Science, Swiss Federal Institute of Technology (ETH), LAPETH, HPP J7
CH-8093 Zurich, Switzerland
jeker@atmos.umnw.ethz.ch
staehelin@atmos.umnw.ethz.ch

[2] NASA Ames Research Center,
Moffett Field, CA 94035-1000, USA

[3] KNMI (Royal Netherlands Meteorological Institute), Section of Atmospheric Composition, P.O. Box 201, 3730 AE De Bilt, The Netherlands

[4] Global Hydrology and Climate Center, NASA / MSFC HR-01 Marshall Space Flight Center, AL 35812, USA

[5] Joint Center for Earth System Science, Department of Meteorology, University of Maryland, College Park, MD 20742, USA

[6] NASA, Goddard Space Flight Ctr, Atmospheres Lab, Code 916, Greenbelt, MD 20771, USA

[7] Solar-Terrestrial Environment Laboratory, Nagoya University, Toyokawa, Aichi, 442-8507, Japan

ABSTRACT

In the framework of the project POLINAT 2 (Pollution in the North Atlantic Flight Corridor) we measured NO_x (NO and NO_2) and ozone on 98 flights through the North Atlantic Flight Corridor (NAFC) with a fully automated system permanently installed aboard an in-service Swissair B-747 airliner in the period of August to November 1997. The averaged NO_x concentrations both in the NAFC and at the U.S. east coast were similar to that measured in autumn 1995 with the same system. The patchy occurrence of NO_x enhancements up to 3000 pptv over several hundred kilometers (plumes), predominately found over the U.S. east coast lead to a log-normal NO_x probability density function. In three case-studies we examine the origins of such plumes by combining back-trajectories with brightness temperature enhanced (IR) satellite imagery, with lightning observations from the U.S. National Lightning Detection Network (NLDN) or with the Optical Transient Detector (OTD) satellite. For frontal activity above the continental U.S., we demonstrate that the location of NO_x plumes can be well explained with maps of convective influence. For another case we show that the number of lightning flashes in a cluster of marine thunderstorms is proportional to the NO_x concentrations observed several hundred kilometers downwind of the anvil outflows and suggest that lightning was the dominant source. From the fact that in autumn the NO_x maximum was found several hundred kilometers off the U.S. east coast, it can be inferred that thunderstorms triggered over the warm Gulf Stream current are an important source for the regional upper tropospheric NO_x budget in autumn.

1. 1 Introduction

Nitrogen oxides (NO_x) near the tropopause lead to ozone production, which is an efficient greenhouse gas at these altitudes [*Fishman et al.*, 1979; *Lacis et al.*, 1990]. The magnitude of the in-situ ozone production following the release of NO_x close to the tropopause critically depends on the existing background NO_x concentration [*Ehalt et al.*, 1995; *Schumann*, 1997; *Wennberg et al.*, 1998]. Since the number of air traffic passenger kilometers is increasing globally by about 5-6 % per year and the related fuel consumption by about 3 % [*Schumann*, 1997], concern about the associated NO_x emissions has been raised. This lead to the compilation of several air traffic emission inventories [*Gardner et al.*, 1998, *Baughcum et al.*, 1993] which are now considered fairly reliable. However, at cruising altitude there are other sources of NO_x for which it is much more difficult to achieve trustworthy quantitative estimates since they are intrinsically linked to meteorological processes, which are not yet fully understood. These sources include the in-situ production from lightning discharges, convective injection of anthropogenic pollutants in thunderstorms and the downward transport from the stratosphere. *Lee et al.* [1997] published a survey of "best" NO_x source estimates, their uncertainties and emission locations. They concluded that lightning is globally the most important source of NO_x but that the estimates are still uncertain (ranging from 2 to 20 $Tg(N)\ yr^{-1}$).

Until recently, the NO_x concentrations at cruising altitude had only been determined during a few episodic campaigns using dedicated research aircraft, which have the ability to carry personnel who operate elaborated chemical analyzers, but the campaigns were typically of short duration.

Brunner [1998] closed this data gap for international air corridors by conducting the first systematic NO_x measurements from aboard an in-service Swissair B-747 in the period of May 1995 to May 1996 in the project NOXAR (Nitrogen Oxides and Ozone along Air Routes). These automatic measurements took place between Zurich, Switzerland, and routes to Far East destinations and on the North Atlantic passage and lead to a tenfold increase of the globally available data set of simultaneously measured NO_x (NO and NO_2) and ozone concentrations at these altitudes.

Brunner et al. [1998] could show that a rather surprisingly large number of extended NO_x plumes exists at cruising altitude, which is particularly pronounced at the U.S. east coast. In summer, these plumes were observed downwind of convective areas, mainly located over the continent. Convective events typically occurred 0.5 to 2 days prior to the measurements since flying directly through active thunderstorms is usually avoided by the pilots. During the other seasons, NO_x plumes were observed predominantly downwind of frontal systems. These findings put previous studies in a more general context: It had been noted before, that such plumes could be attributed to convective motion which can inject large amounts of NO and other ozone precursors from the polluted planetary boundary layer to the cruising altitude of commercial airliners [*Chatfield and Crutzen*, 1983; *Dickerson et al.*, 1987] and to lightning discharges which produce NO [*Liebig*, 1827; *Raizer*, 1967; *Goldenbaum and Dickerson*, 1993]. *Biazar et al.* [1995] published estimates of the summertime NO_x production from lightning over the United States using flash rates gathered from the National Lightning Detection Network (NLDN). By comparing these estimates to anthropogenic emissions from the National Acid Precipitation Assessment Program (NAPAP)

inventory, they concluded that this natural source cannot be dismissed relative to anthropogenic sources even though the uncertainties in actual emission factors are large.

Huntrieser et al. [1998] compiled a comprehensive survey of previous studies on transport and production of NO_x in electrified thunderstorms. They note that only a limited number of in-situ studies with anvil penetrations have so far been carried out, predominantly over the American continent [*Ridley et al.*, 1987; *Frantzblau and Popp* 1989; *Luke et al.*, 1992] and the Pacific Ocean [*Chameides et al.*, 1987] and therefore performed the first anvil penetration missions over Germany and Switzerland with the DLR Flacon in the field campaign LINOX (lightning produced NO_x) [*Huntrieser et al.*, 1998; *Höller et al.*, 1999]. The EC sponsored EULINOX (European Lightning Nitrogen Oxides Project) program continued these research efforts during the summer of 1998. These projects are expressions of the compelling need to better understand the mechanisms of lightning produced NO_x and to get better estimates of the importance of the lightning source.

The coordinated European and American programs POLINAT-2 (Pollution in the North Atlantic) and SONEX (SASS Ozone and Nitrogen Experiment), performed in autumn 1997 in the North Atlantic Flight Corridor (NAFC), are the latest efforts of a series of campaigns aiming at getting a better understanding of the impact of aircraft emissions [*Schumann et al.* this issue; *Singh et al.*, 1999; *Thompson et al.*, 1999]. While the DLR Falcon and the NASA DC-8 performed high precision measurements of a large spectrum of chemical parameters, the NOXAR system aboard the Swissair B-747 systematically measured the distribution of nitrogen oxides (NO and NO_2)

and ozone during 98 traverses of the North Atlantic in the period of August 13 to November 23, 1997 [*Jeker et al.*, 1998].

By presenting three case-studies, we will show that the location of measured large scale NO enhancements can be well explained with the combined application of back trajectories, satellite observations of both clouds and lightning activity as well as ground based lightning observation systems. For cases of marine convection, for which the anthropogenic component to the NO enhancements is hence of minor importance, we will show that the number of lightning flashes occurring in a cluster of convective clouds correlated well with the NO concentration enhancements measured a few hundred kilometers downwind of the thunderstorms. In the third case-study we report an NO plume over the North Eastern Atlantic and attribute it to lightning discharges observed by the Optical Transient Detector (OTD) satellite. Finally we will give an overview over all measurements that we carried out during POLINAT 2 and relate the results to the given evidence of lightning produced NO.

2. Measurements and methods

2.1 Chemical measurements

The measurements during POLINAT 2 were performed with the completely automated NOXAR device for the measurement of NO, NO_2 and O_3, which was permanently installed in the cargo bay of a in-service Swissair B747-357 described in *Brunner* [1998] and *Dias-Lalcaca et al.*

[1998]. Here we only briefly discuss the most important modifications carried out for the POLINAT 2 campaign. A more detailed listing can be found in *Jeker et al.* [1998].

2.2.1 NO_x measurements and calibrations

The NO and NO_2 measurements were performed with two identical Eco Physics 780 TR chemiluminescence detectors. NO_2 is converted to NO using the Eco Physics PLC 762 photolytic converter upstream of the second chemiluminescence detector.

The drift of the zero signals of the instruments during each flight as well as laboratory measurements which showed that the zero signal is also function of the humidity in the sample gas, lead us to use a humidifying unit as well as a new calibration type making use of the device's integrated pre-chamber. In this calibration, an excess amount of ozone is added to the sample gas in the pre-chamber, where 95 % of the NO reacts in a chemiluminescent reaction, before it reaches the main chamber where the photon detection takes place. The remaining 5 % of NO leaving the pre-chamber are accounted for by using the mean NO concentration measured before and after the calibration, to estimate the NO content of the sample air during the calibration. Only calibrations with stable NO content in the preceding and following measurement cycles were considered. Through frequent calibrations (every 2 minutes during 30 seconds) the temporal evolution of the instruments' zero line could be accurately determined and good confidence in the measurements gained. The mass-flow controllers of the Environics S-100 system used for inflight sensitivity calibrations of the analyzers were calibrated and in consequence the inflight NO-calibrations corrected by +7 %. The overall precision and accuracy of the instrumentation are

comparable to that described in *Brunner* [1998]. In order to asses the performance of the entire system in air, we performed an intercomparison flight where the DLR Falcon followed the Swissair B-747 in the Shanwick- radar control zone for about 15 minutes. It was concluded that although the conditions for the intercomparison were unfavorable, due to crossing of many aged aircraft plumes by both the Falcon and the B-747, the NO measurements agreed well within the combined errors [*Ziereis et al.*, 1998; *Jeker et al.*, 1998].

Due to the persisting difficulties in measuring the low NO_2 concentrations at day time, we calculated the photostationary state equilibrium concentration based upon measured NO and O_3 concentrations as described in *Brunner* [1998]. The sum of measured (day-time) NO and calculated NO_2 shall be labeled NO_x^* throughout this paper. At night time, when NO_x is fully converted into NO_2 due to the titration of NO with O_3, the measured NO_2 concentrations can be used semi quantitatively to trace NO_x plumes.

2.1.2 Ozone measurements

Ozone is measured with an Environics S-300 UV absorption device. Laboratory measurements before the campaign suggested that some bias in the (pseudo) vertical profiles, obtained during the NOXAR 1995/96 project could possibly be caused by humidity interference [*Meyer et al.*, 1991] occurring in the UV absorption tube. These examinations lead us to retrofit the instrument with the original Teflon coated ozone absorption tube, with which this effect could be minimized in the laboratory. At the end of the campaign we calibrated the ozone analyzer against the primary NIST-14 ozone reference instrument at the Swiss Federal Office for Standards (EAM).

Moreover we applied a correction of +6.5 % to all ozone measurements to account for losses in the sample lines and the ozone compressor. The correction factor was determined experimentally on ground before the system was removed from the aircraft and no significant (simulated) altitude dependence of this factor could be found. During the above mentioned intercomparison flight agreement within the combined errors of the instrumentation was found [*Ziereis et al.*, 1998; *Jeker et al.*, 1998].

2.2 Tools for the interpretation of the data

2.2.1 ECMWF fields and kinematic trajectories

We made extensive use of three dimensional kinematic back trajectories calculated with the software package "Lagranto" [*Wernli and Davies,* 1997]. As the input for the calculations we used analyzed meteorological fields of the European Center for Medium-range Weather Forecast (ECMWF) (T213/L31). The trajectories were started at the closest full hour and calculated with an integration time step of 30 minutes. The same fields were also used for interpolating meteorological parameters such as potential vorticity (PV) in space and time along the flight tracks. Several studies have shown that different types of trajectories may exhibit significant spatial position errors [*Stohl et al.*, 1997; *Selkirk et al.*, this issue] and care must therefore be taken when particle motions are interpreted. For each individual case-study presented below, we therefore assessed the quality of the ECMWF meteorological fields by comparing the measured aircraft parameters to the respective model parameters along the flight track. This prevents us

from using inaccurately analyzed fields - which we found in rare cases on flight legs over remote areas such as Siberia. However, for practically all flights of the campaign, the data of the ECMWF fields was in good agreement with the wind and temperature measurements obtained from the standard sensors of the B-747 (Figure 1), which makes these meteorological fields a valuable tool for analyzing the synoptic motion of air masses at commercial airliner's cruising altitude.

2.2 Aircraft influence along the flight track

We estimated the concentration increase, which can be attributed to aircraft emissions, by combining the information from backward trajectories with the 3D aircraft emission database ANCAT/DLR-2 [*Gardner et al.*, 1998]. As input we used the database at T42 horizontal and 1 km vertical resolution. The database represents worldwide civil air-traffic emissions from July 1991 (estimated to $1.37388 \cdot 10^8$ kg NO_2 globally).

The ANCAT emission rates in each grid box given as mass emitted per time were first converted into emission rates in terms of concentration increase per time by assuming a homogeneous distribution in the grid box. Then, we summed up these emissions at each position along the calculated trajectories over the previous 5 days. We also applied 3 different artificial lifetimes of NO_x (3d, 5d, ∞) in order to reduce the weight of emissions which occurred further back in time. The data are based on optimum flight profiles and flight tracks (great circles) and do not take into account any Air Traffic Control (ATC) delays. Furthermore the database does neither include a diurnal cycle of air traffic loads nor have we accounted for the North-South shifting of the entire

corridor which is done in order to optimize the flight tracks with respect to the actual position of the jet-stream. Therefore, the calculation can only provide a rough estimate. Nevertheless, we expect the method to be able to identify air masses which were exposed to air traffic emissions over anomalously short or long periods of time. For the cases presented in this paper, very low values of between 0 to 50 pptv were typically found in the Eastern Atlantic. These low values could often be explained by air masses which stayed in the North Atlantic Flight Corridor (NAFC) for only a comparatively short period of time and which had a previous history with little air traffic emissions, as is the case for polar air streams. At the U.S. east coast the analysis often revealed significant concentration increases up to 250 pptv, (assuming a NO_x lifetime of 10 days). This reflects the emission outflow from the rather dense domestic U.S. air service system (Figure 2), which is in line with a study of *Witte et al.* [1997], where large scale enhancements in NO/NO_y measured during the AASE-2 campaign were attributed to air-traffic taking place over the eastern United States. Another result of our estimates is that strong gradients of the aircraft attributable NO_x existed even on neighboring flight legs (Figure 2). Such gradients could often be explained by rapidly occurring changes of the predominant flow regimes, which carried air with different histories of air-traffic exposure to the NOXAR flight track. Since we only investigated the effect for the three case-studies presented here, we do not claim this to be representative for other days. But the analysis shows that it is necessary to examine each individual case and that generalizations without climatological trajectory studies might be fairly difficult to achieve. A similar remark has already been made by *Witte et al.* [1998] where difficulties in using climatological NO_x emission data bases to infer instantaneous NO/NO_y ratios were reported.

2.3 Lightning observations

We used both data from the U.S. National Lightning detection network (NLDN) and from the Optical Transient Detector Satellite (OTD) to explore the history of lightning encounter of plume air masses (all data were kindly provided by the Marshall Space Flight Center (MSFC)). The NLDN provides lightning data covering the continental United States since 1989 from an array of more than 100 sensors detecting ionospherically propagated electromagnetic signals from cloud-to-ground lightning discharges. Recent assessments showed that for our application the system has a very high median location accuracy of about 500 m. The expected flash detection efficiency for continental thunderstorms ranges from 80% to 90% for those events with peak currents above 5 kA, varying slightly by region [*Cumnis et al.*, 1998; *Idone et al.*, 1988; *Wacker and Orville, 1999*]. Although the detectors are positioned on the North American continent, the data of this system can also be processed to detect lightning occurring at sea. However the detection efficiency of this long range network decreases strongly with increasing distance from the shore. By comparing observations from different locations within the U.S. arrays and by carrying out joint trans-Atlantic experiments involving sensors from Meteo France, *Cramer et al.* [1998] could show that for the observations of several marine thunderstorms the detection efficiency was about 20 % at local night but it dropped to only a few percent during local day time.

For lightning occurring in remote areas, such as the mid North Atlantic, it is necessary to use satellite observations. The OTD satellite has been continuously monitoring global intracloud and cloud-to-ground lightning from a near-polar orbit since April 1995 [*Christian et al.* 1996]. The

instrument is comprised of a 128x128 CCD pixel array, with individual pixel resolutions from 8-13 km across, and a total field of view of 1300x1300 km^2. The OTD sensor attitude (orientation) may rotate over the course of an orbit, so individual geographic locations may be observed from anywhere between 1 and 270 seconds. Lightning detection can be achieved with a detection efficiency of about 55 to 70% [*Boccippio et al.*, 1999]. However, the satellite is a climatology, rather than storm-scale observation instrument and is not designed for high location accuracy; nonetheless, careful examination of the satellite data can usually provide an estimate of the location errors at any given time.

2.4 Tracing convective and lightning influence

Large scale models often have difficulty predicting the exact location and intensity of convective events. Thus, in order to evaluate the impact of convection on the distribution of trace constituents such as NO and NO_2, it is useful to use high resolution satellite imagery to locate convection. In fact, combining GOES-8 and Meteosat imagery with model trajectories, enabled *Brunner et al.* [1998] to come to the above-mentioned conclusions regarding NO_x plumes. In order to verify whether high concentrations of surface or lightning produced NO_x were carried to the altitude of the back trajectories originating in large NO plumes, we used the cloud top brightness tracing method [*Jeker et al.*, 1998] in which the cloud top temperatures are traced along the trajectories and compared to their temperatures.

Given the big impact that the combined effects of convection and lighting events have on the regional NO_x budget at the U.S. east coast have, convective- and lightning influence plots were

extensively used for SONEX flight planning [*Thompson et al.*, 1999]. In their approach isentropic back trajectories from a 1 by 1 degree area of points are calculated using the GSFC GEOS-1 analyses. The potential temperature surface is selected to correspond closely with the potential temperature at the aircraft's locations. Each trajectory is then examined for evidence of convective/lightning influence by verifying its proximity to cold satellite brightness temperatures and observed lightning. Convective/lightning influence is said to occur at some point along the trajectory if:

(a) the brightness temperature is no more than 5 K warmer than the parcel temperature along the trajectory; (b) lightning has been observed within 3 hours of the time the satellite image was taken; and (c) the parcel is not in the stratosphere (defined as an Ertel Potential Vorticity of greater than 3.25 PVU). The result is a 1 by 1 degree "map" of convective influence containing: (1) the time to the most recent convection and (2) the number of lightning flashes observed during the most recent convective encounter. No attempt is made to examine the convective history prior to the most recent convective encounter (since the isentropic trajectories are almost certainly unreliable at such times). In no case are the trajectories taken back more than 5 days, since NO_x decays in the upper troposphere on a 1 week or so time scale. The details of the scheme are described in *Thompson et al.* [1999], along with the potential sources of error. However, for our purposes the most likely source of error is the 3-hourly satellite time resolution combined with 6-hourly lightning accumulations. Essentially, some of the lightning flashes in a 6-hourly period may not be "counted" as having an effect on the upper tropospheric trajectories because the 3-hourly "snapshot" does not happen to contain cold cloud. This sort of error should

be less important for the longer-lived frontal convection discussed by *Brunner et al.* [1998]. (Examples of convective influence plots can be found in Figures 4a to c.)

3 Results and discussion

3.0 Comparing model products and measurements

In order to compare the NO measurements to the maps of convective influence, we proceeded in two steps: We first subtracted the estimated aircraft concentration enhancement which we obtained with the above mentioned method in which back trajectories are combined with the ANCAT emission database. This approach assumes that homogeneous mixing of the emissions in each grid has already taken place. In a second step we therefore filtered out the short NO spikes which can be attributed to the crossing of young aircraft exhausts [*Schlager et al.*, 1996], and which have therefore not yet been homogeneously mixed.

In addition to the already mentioned simplifications of the ANCAT tracing approach, two other simplifications of this approach become apparent: By subtracting both the young aircraft spikes and the averaged ANCAT database concentrations, we do a double counting for the period of time until the spikes are not anymore statistically discernible from the background concentrations. The other error comes from the fact that the ANCAT database tracing should ideally be stopped after a first convective encounter, after which the back trajectories become unreliable. Both error sources therefore potentially lead to an overprediction of the aircraft influence.

Nevertheless the residing is an approximation for the sum of all NO_x sources other than aircraft. For cases where no significant downward transport from the stratosphere took place and where no large (gas phase) chemical in-situ production took place, this difference represents the combined effects of convective injection of NO_x from the planetary boundary layer and the production of NO_x in lighting discharges.

3.1 First case-study: Frontal activity over the Eastern United States

A series of large NO_x plumes which we observed at the U.S. east coast on several consecutive days between September 11 and 13, 1997 are described here along with an interpretation of their origins. Early during September 10, an elongated PV streamer moved slowly towards the eastern part of the North American continent over a region characterized by a moderate north-south temperature gradient. Only a weak surface cyclone formed near the leading edge of the streamer and reached the eastern part of the Great Lakes at 1200 UTC on September 11 (Figure 3a). The PV streamer induced strong low-level northerly flow of warm moist air along its eastern flank and triggered convection just behind the American east coast. Note also the high CAPE (Convective Available Potential Energy) values along the coast (Figure 3b) - a region where high lightning frequencies were observed by the NLDN. In the upper panel of Figure 4a it can be seen that the highest NO_x concentrations were observed at the U.S. east coast on the NOXAR east- (not shown) and westbound flights on September 11. The maps of convective influence clearly distinguish the area without convective influence (black) from the convective outflow (colored) from the above mentioned frontal system, which is in good agreement with the measured

concentrations. As these convectively influenced air masses have been transported further East (see map in Figure 4b) we encountered again, another although less pronounced NO plume, between 50 and 70° W on September 12. Note how the sharp concentration drop at the western edge of the plume is also represented in the map, altough it underpredicts the eastward extension of this plume. As mentioned above, only lightning accompanied convection is considered in the maps. An underprediction might therefore be explained by vertical transport of polluted continental planetary boundary layer, in clouds which did not exhibit lightning activity. The map for September 13 (lower panel in Figure 4c) shows, that the frontal system stretched even further out into the Atlantic on that day, which lead to sampling of enhanced NO concentrations between 40 and 70° W, although the enhancement was less pronounced than on the previous days.

In Figure 5 we make (with the data of these four flights) a more quantitative approach to demonstrate the method's ability to automatically separate air masses with and without a history of recent convection. The confidence intervals (notches in the boxplots) of the median values of the data sets with and without convective history, do not overlap which portrays a statistically significant median difference between the two groups. It is thus possible to reliably detect the location of convection with an automatic algorithm. However, the scatter of the NO_x measurements with a recent convective encounter is much larger. This is to be expected, since the only separation criterion was convective history and we did neither consider different exposures to continental pollution and lightning discharges nor the time at which the NO_x loading took place.

The scatter of the data, and with it the confidence intervals of the median values, can be further reduced when we subtract the aircraft influence from the data (as mentioned in part 2.2 of the paper). This shows that both (convection and aircraft) exhausts are factors which help to explain the NO_x budget on these four flights.

Last but not least, the boxplots from these four flights illustrate the order of magnitudes of the different factors affecting the NO_x budget at cruising altitude and the scatter which is introduced by these factors. For instance the large scatter of the data with a convective history would make it statistically infeasible to separate the comparatively small aircraft contribution from the noisy background (see also *Thompson et al.*, 1999). On the other hand for the estimation of the aircraft contribution, it would be venturesome to only consider data sets without this problem (i.e. without a convective history) and generalize these results: Upon approach at the U.S. east coast the probability of encountering convectively influenced air masses increases simultaneously with that of encountering recent aircraft emissions from the rather dense U.S. domestic air services.

We therefore conclude that the location of convectively influenced air masses can be accurately determined using an automated algorithm. However, in order to be able to isolate the comparatively small aircraft signal from convectively influenced air masses, the scatter of the data would have to be removed. This goal could be achieved by reducing the number of relevant sources for the NO_x concentration at cruising altitude (such as pollution from the planetary boundary layer) and by introducing new explanatory variables (such as the number of lightning flashes and the time since most recent convection) to describe the NO_x budget.

3.2 Second Case-study: U.S. East Coast Lightining Activity on November 09, 1997

For cases of marine convection, the vertical transport of anthropogenic NO_x is of lesser importance, so that the contribution from lightning discharges gains weight for the regional NO_x budget at cruising altitude. We found such a situation on November 9, 1997 when SONEX performed the first cross-corridor measurements out of Bangor Maine, and the NOXAR system was operated between Zurich and Atlanta. A horizontal and vertical section of all flights is given in Figures 6a and b, respectively. We will focus on the measurements which were performed in a well developed frontal system resulting from a classical, although moderate case of east coast cyclogenesis taking place between November 7 and 10. An elongated zone of strong baroclinicity extended zonally from Florida to the central Atlantic at 1200 UTC on November 7 (Figure 7a). A surface cyclone formed below the leading edge of an almost circular positive upper level PV-anomaly at that time. The cyclone intensified and established a T-bone frontal structure (Figure 7b and Figures 8a and b) where the temperature contrast associated with the warm front was much stronger than for the cold front.

Until shortly before reaching the U.S. east coast, the NOXAR westbound flight took place in the lower stratosphere where background NO concentrations of about 100 pptv were sampled (section 3 in Figures 6a and b). At about 40° W, the ozone concentration dropped from its initial level of about 120 ppbv to 70 ppbv as soon as the aircraft entered the upper troposphere, where all remaining measurements were performed. But only about at 50° W km, a prominent NO plume was encountered between 1445 and 1800 UTC (sections I-III in Figure 9 and section 1 in Figures 6a and b). Such sharp horizontal NO gradients in the troposphere could rarely be

observed during POLINAT-2. Most often sharp horizontal NO_x gradients could be explained by the aircraft's passage from the stratosphere to the troposphere, where the maximum NO_x concentrations can be much higher than in the lowermost stratosphere. Figure 9 shows that also the SONEX aircraft, which started sampling the same area with a time lag of about one hour, detected highly variable NO concentrations with maxima of up to 3000 pptv between 1800 and 2100 UTC. The most prominent NO enhancements were constrained to the cross-corridor flight legs at altitudes higher than 8.5 km between 53.5° and 57° W (section 2 in Figures 6a and b). Last but not least on the respective eastbound flight at night (about 0300 UTC) the NOXAR aircraft sampled NO_2 concentrations in excess of 3000 pptv downwind of the area where SONEX detected the highly variable NO concentrations (section 3 in Figures 6a and b).

With the "ANCAT tracing method" we found that the aircraft attributable NO varied significantly along the entire flight (Figure 2) but never exceeded values of 250 pptv. Thus, although this source is not negligible, it can barely explain 10 % of the high NO concentrations measured in the plume.

The air masses on the NOXAR flight leg before the NO plumes were encountered, previously crossed the American continent at cruising altitude (section 1 in Figures 6a and b). These low NO concentrations can be explained by the clean polar air into which not much aircraft exhaust was emitted and which, according to the results of the "brightness tracing method", did not undergo recent convection. In contrast to these air masses, the kinematic ECMWF back trajectories starting on the NOXAR west- and eastbound flights and on the SONEX flight legs where highly elevated NO concentrations were observed, belonged to a significantly different flow regime, in

which the air followed an upper level trough associated with the previously described surface low pressure system (sections A to C in Figure 6a). (Other cases with elevated NO concentrations and a similar flow pattern were detected on SONEX flights 10 and 12, which took place on October 29 and November 3 respectively [*Thompson et al.*, 1999]).

On the passage over the Atlantic, the back trajectories originating in the NO_x plumes crossed an area of intense lightning activity (contours in Figure 6a) which was observed by the U.S. National Lighting Detection Network (NLDN) long range channel. During the period of time (2100 to 2300 UTC on November 8) which is depicted in Figure 6a, heavy thunderstorms in the highlighted area exhibited more than 1900 cloud-to-ground flashes (about 15 flashes per minute). This number, however, must be seen as a lower limit, due to network's exponentially decaying detection efficiency of the long range channel, with increasing distance from the shore [*Cramer et al.*, 1998]. Superimposition the data from the lighting detectors on the brightness temperature enhanced GOES-8 satellite images, and the production of animations of these composites, revealed good agreement between the location of the highest convective cells and the corresponding trajectories in the time period of ten hours prior to the observed NO plumes. The brightness tracing method suggested, that these thunderstorms were high enough to inject NO_x into the above crossing air masses (section C in Figure 10).

By discussing the structure and the history of the NO plume observed on the NOXAR westbound flight in more detail, we will show that large fractions of the concentration enhancements can most probably be attributed to lightning activity. Essentially the entire plume, which was

observed in the longitude range of 50 to 67° W, can be subdivided into three sub-plumes (I to III in Figure 9) with marked concentration gradients at about 57° W and 61° W.

The back trajectories starting in the first sub-plume experienced significant convective influence for the first time between 15 to 20 hours prior to the measurements. Interestingly, some of the relevant thunderstorms, which were not accompanied by lightning activity, developed over the heavily polluted continental area between Boston and Philadelphia which apparently did not cause very strong NO concentration enhancements at cruising altitude. Prior to that, some trajectories crossed a number of isolated convective clouds at sea, which all exhibited low lightning frequency.

The concentrations during the second and most prominent sub-plume reached levels of up to 3000 pptv (section II in Figure 9), when the aircraft flew over the wider area of Newfoundland between about 1515 and 1545 UTC. The corresponding back trajectories crossed Nova Scotia, descended the Gulf of Maine and experienced the first convective encounters at sea, about 11 hours prior to the plume observation, in convective clouds which exhibited higher lightning frequencies. The air mass then moved further South and at -18 hours it was fully immersed in a cluster of convective clouds (squares in Figure 8a), all of which still exhibited very strong lightning activity. The southernmost trajectories then left the cloud cluster again at about –21 hours and no convective influence occurred prior to 27 hours before the plume observation was made. On average these air masses were exposed to stronger lightning activity and exposure also occurred over longer periods of time (4 to 6 hours) than the air masses sampled during the first sub-plume.

In a quantitative analysis, we therefore summed up the number of lightning flashes to which the trajectories starting on the flight track were exposed during their most recent encounter (Figure 11a). The first sub-plume was exposed to about 100 to 150 flashes. In Figure 9 it can be seen that it was separated from the next sub-plume by very low NO values – the back trajectories of which were not exposed to significant lighting activity. The air masses of the second sub-plume were exposed to roughly a three times higher number of flashes. This number correlates well with the NO concentrations measured on this flight leg (note that all lightning flashes mentioned above have not been corrected for the detection efficiency of the NLDN LR channel). This suggests a linear relationship between the number of lightning flashes that an air mass encountered and the resulting NO concentration. The good correlation is an indication for the lightning origin of this large scale plume. Even more interesting is the fact that the big concentration gradients are conserved still several hundred kilometers downwind of the cluster of thunderstorms.

To further strengthen evidence for the lighting hypothesis, we started ECMWF back trajectories from a 1x1 degree grid at different pressure levels (400, 600, 800, 900 hPa) covering the area between 65 to 75° W and 30 to 45° N (dotted rectangle in Figure 6a) to test whether polluted low level continental outflow, could have been lifted to the altitude of our trajectories of interest in the marine convective systems described above. For the three upper levels, we find no evidence of such motion (Figure 12) although for the 900 hPa level there are several trajectories where the air crossed the polluted U.S. continent in the period of 1.5 to 3 days before convection occurred over the ocean. Due to the very short lifetime of NO_x at these low levels [*Jaeglé et al.*, 1998], we

believe that by the time when polluted continental outflow had reached the bases of the convective clouds, large fractions of the initial NO_x concentrations must have decayed.

The chemical tracer measurements aboard the DC-8 suggest that the above mentioned lightning activity occurring at sea must have played an important role for explaining the high NO levels encountered during the SONEX cross-corridor flight stack. The CO concentration remained between 90 to 100 ppbv which is an indication for a rather small fraction of polluted boundary layer air. The hydrocarbon measurements, especially the typical tracer for anthropogenic emissions, acetylene, remained at relatively low levels of between 70 to 140 pptv. The same goes for the other non oxidized tracer species such as propane (40 to 200 pptv) ethane (600 to 900 pptv) and methylbromine (9 to 13 pptv). The high NO/NO_y ratio up to 0.7 in large parts of the cross-corridor flight stack provides evidence for fresh NO emissions.

On the westbound return and especially during the last flight leg immediately prior to final descent, traces of moderate anthropogenic surface pollution were found in increasing concentrations. On this flight section propane and acetylene tripled, ethane nearly doubled, while tetrachlorethylene [*Snow et al.*, this issue] and CO significantly raised while the NO_y concentration decreased when the aircraft descended. (The only exception are convective cells containing lightning just a few minutes transport time south of the SONEX flight track over the southern part of the Canadian province of New Brunswick which likely contributed to these enhancements [*Pickering et al.*, this issue]). Even on this flight section where anthropogenic pollution was important, the anthropogenic emissions therefore only moderately affected the NO budget at cruising altitude. Significant upward transport of pollutants would possibly also have

resulted in NO concentration enhancements at lower levels. Figure 6b shows that this was not the case and that the highest NO concentrations could be found close below the tropopause (not shown).

We conclude that the strong lightning activity, a few hundred kilometers off the U.S. east coast, influenced the NO budget along the flight track of the NOXAR westbound on November 9 very significantly. Hence we saw that the back trajectories starting on SONEX flight legs with similarly high NO concentrations followed comparable paths as those starting in the NO_x plumes observed on the NOXAR west- and eastbound flights. These results are in line with a number of other publications dealing with the SONEX November 9 flight for which *Thompson et al.* [1999] gives an overview. *Allen et al.* [this issue] found, based upon NO_y tracer simulations, that the SONEX flight performed on November 9 was the one which was most dominated by the lightning source (at least half of total NO_y) and *Pickering et al.* [1999] compared this flight to the November 3 SONEX flight which also contained significant lighting sources.

The warm Gulf Stream sea surface temperatures of 20-25° C (section B in Figures 7a and 10, see also *Pickering et al.* [this issue]) most probably played an important role in triggering convective clouds that are accompanied by lightning discharges, which produce large NO_x concentration enhancements that are carried close below the tropopause. This is a result that could be further generalized taking into account evidence by *Orville et al.* [1990] who have shown that for winter lightning activity there is a close correlation between the maximum lightning intensity contours with the maximum sea surface temperatures. Using PV as an additional tracer for air parcel origins confirms the strongly subtropical signature of the SONEX observations and points to

lightning (with some surface pollution) as the major NO_x source during the SONEX mission [*Thompson et al.*, 1999]. The strong lighting activity at the U.S. east coast might therefore also explain the large number of NO_x plumes off the U.S. east coast which were observed in autumn and winter of 1995/96 [*Brunner*, 1998] and during the POLINAT-2 campaign in autumn 1997 [*Jeker et al.*, 1998].

3.3 Third case-study: Marine convection and lightning on August 14, 1997

In remote areas such as the North Eastern Atlantic, it can be assumed that the base of a convective cloud is in relatively clean air [*Schiff et al.*, 1979, *Helas et al.*, 1981] and that upward transport of air is therefore not accompanied by the injection of a large amount of pollutants. Here we present such a case of marine convection and will give evidence, based upon several satellite observations, that the for this location unusually high NO concentrations downwind of convective systems can be attributed to lightning discharges.

On the flight from Zurich to Atlanta on August 14, 1997 a NO plume extending about 1000 km, along the flight track was encountered over the North Eastern Atlantic between 7.5° W/47.5° N and 25° W/60° N (Figure 13 and flight track in Figure 14b). During the 70 minute (1100-1210 UTC) plume encounter, three sub-plumes are identifiable which each exhibit peak concentrations in excess of 800 pptv (2 minute average) and which are separated by local minima of about 400 pptv. Although the measurements from the entire flight are given in Figure 13, we will only concentrate on the first large plume since the elevated NO_x levels upon approach at the U.S. east coast are a feature that was already covered in the two previous case-studies. Along a discussion

of the predominant meteorological situation, this case-study aims at identifying possible sources of these high NO concentrations for at this time of year rather untypical location.

Ryall et al. [1998] described cross-Atlantic transport of long-lived gases such as CFCs which were emitted over the United States and detected at Mace Head, Ireland in a study in which they explained measurements with a tracer simulation. Long range transport of NO_x from the U.S. east coast therefore potentially needs to be considered as a source, although for NO_x the situation is largely different from that of the CFCs, in that NO_x has a comparatively short atmospheric lifetime of between 4 to 10 days at cruising altitude [*Jaeglé et al.*, 1998] and Table 1. In the case of relatively weak marine convection, it is possible that not the entire airmass downwind of a convective system originated in the marine boundary layer but rather that it can be seen as a mixture of the existing NO_x concentration at cruising altitude, which may occasionally contain significant amounts of pollutants from surface sources, NO produced in the thunderstorms and clean air from the marine boundary layer, which may dilute the high NO concentrations.

The high NO measurements were performed in a cyclone which developed on August 9 South East of Greenland below a prominent filamentary upper-level PV feature. It reached maturity one day later, remained almost stationary and decayed very slowly during the next 5 days. At 0000 UTC on August 11 the upper-level development led to a cut-off (Figure 14a) which co-evolved with the surface cyclone as a near-barotropic vortex. Between 0600 UTC on August 13 and 1800 UTC on August 14 convection was triggered on several occasions by the rotating PV-anomaly in regions characterized by high values of relative humidity in the lower troposphere. Figure 14b, shows the shape of the PV cut-off at the flight level (~325K) at 1200 UTC on August 14. The

initial flight leg in the tropopause belongs to the high NO_x plume, whereas the NO_x concentrations rapidly decreased when the airplane entered the cut-off of stratospheric air at about 25° W shortly after 1200 UTC which is also marked by a steep increase in the measured ozone concentrations. This is consistent with the low pressure altitude of the ECMWF tropopause; the PV2 and PV4 levels extended down to 370 hPa and 350 hPa respectively (Figure 13).

Kinematic back trajectories based upon ECMWF analysis data were started at two minute intervals along the flight track inside the NO plume in order to identify its possible sources. The back trajectories starting in the first sub-plume exhibit motion in an almost stationary cut-off low (Figure 15a) over the ocean. They oscillated within a band of ± 1 PVU around the tropopause (2 PVU) during the previous 60 hours and remained to the east of 51° W during that period of time. Prior to that the trajectories descended from the stratosphere where they remained in the range of 2-7 PVU for a period of about 40 hours. The low tropopause therefore most likely prevented any convection from carrying urban pollution to the trajectories. The trajectories starting in the two following sub-plumes exhibited very similar motions and based upon brightness temperature tracing plots and animated GOES-8 images we found no evidence that convection over polluted of the the U.S. continent (or over the coast) could have transported significant amounts of anthropogenic NO_x to cruising altitude.

Although 3D kinematic trajectories are the most accurate trajectory type in the troposphere *[Stohl et al.*, 1998], eventual horizontal and vertical trajectory position errors may occur, which would render the brightness tracing information used in the argumentation above invalid. In order to

avoid this potential uncertainty, we estimated the NO_x lifetime over the North Atlantic in our area of interest. Table 1 gives a summary of the 1/e-lifetimes as calculated with the Harvard 0D model [*Jaeglé personal communication*]. It can be seen that the lifetime increases with latitude but decreases significantly with lower altitudes. All trajectories starting inside the plume oscillated in the altitude range of 200 to 300 hPa between 40 and 60° N so that the real NO_x residence time along individual parts of the trajectories can be estimated to lie between 3 and 6 days. This independent analysis therefore also leads to the conclusion that large parts of the extended NO plume must have been produced rather recently and therefore locally.

Although the NO plume observation was carried out in the troposphere, the airmasses have a stratospheric history as indicated by the evolution of the trajectories' PV values. This calls for an evaluation of the possible importance of stratospheric NO_x sources since in cut-off low, events of stratosphere to troposphere exchange are likely to occur [*Poulida et al.*, 1996]. Parts of the NO_x concentration increase during the plume might therefore be attributed to stratospheric NO_y sources as it is known that in the lower stratosphere, there may be a strong correlation between O_3 and NO_y [*Murphy et al.*, 1993]. The stratospheric NO_y budget has also recently received renewed attention by the discovery of a new NO_x source in lab experiments [*Zipf et al.*, 1998]. The authors showed that the photoexcitation of $O_2(B^3\Sigma_u)$ molecules and short-lived collision complexes of weakly bound N_2:O_2 dimers by the absorption of solar Schumann-Runge and Herzberg band and continuum radiation is an efficient source of NO/NO_2 in the stratosphere and possibly the troposphere. This source might be equally important to that of the decomposition of N_2O. However, based upon the averaged NO concentration profiles (scaled with respect to the

tropopause) which were obtained in the North Atlantic Flight Corridor during NOXAR [*Brunner*, 1998] and POLINAT-2 (Figures 18a and b), we believe that the stratospheric influence on the observed NO plume might only be of the order of 200 pptv at most. Another indication that the stratospheric NO source was most probably of minor importance, is the fact that as soon as the aircraft entered the stratosphere (high ozone and PV in Figure 13), the NO_x plume disappeared almost immediately.

Schlager et al. [1997] have reported a series of in-situ measurements inside a static anti-cyclone in which they attribute large parts of the observed NO_x concentration increase to accumulated air-traffic emissions into the North Atlantic Flight corridor. With the method described in part 2.2 of this paper we calculated the contributions of aircraft emissions along individual trajectories starting inside the plume and found that aircraft emissions may only have accounted for maximally 130 pptv when accumulation is assumed to have taken place over the previous five days (i.e. eternal lifetime).

It can be concluded that the sum of the NO concentrations resulting from possible continental outflow from the United States, from stratosphere to troposphere exchange in the cut-off low and from the input of air-traffic is significantly lower than the high NO concentrations observed during the marine plume. It is therefore very likely that these elevated NO levels were produced locally in one or more marine thunderstorms. This hypothesis is supported by the observations of several satellites and the U.S. Long Range (LR) NLDN. Below we give a description of the most important observations (see also Table 2).

Deep convection along the southern flank of the cut-off system described above was observed by the GOES-8 satellite from 0300-1300 UTC 13 August. The brightness tracing plot in Figure 16 shows that the highest clouds reached the altitude of the back trajectories. Cloud tops colder than -50 ° C (near-IR) were also observed by the constellation of DMSP satellites during this window. Four lightning ground flashes were observed by the LR network before sunrise at the U.S. east coast. The LR network was probably unable to detect any flashes occurring after about 0700 UTC due to the transition to local day, due to the very low detection efficiencies at such distances. Lightning observation by the DMSP Optical Line Scan (OLS) sensors was precluded by the far northern latitude of this system: during summer seasons, high latitudes are almost always in daylight when viewed by the DMSP/OLS sensors, which can only discriminate lightning at night.

Based on Optical Transient Detector (OTD) satellite observations, the cloud cluster was infrequently producing lightning as early as 1015 UTC on 970812, and probably continued at this rate until at least 0050 UTC 970813. At about 0300 UTC 970813, GOES IR saw a significant deepening of the convective cells. Consistent with this, the NLDN LR network detected ground flashes between 0442 and 0634 UTC. The coldest cloud tops during this cluster's evolution were observed between 0800-1000 UTC 970813. At 0932 UTC the OTD lightning sensor overflew the convective cells, viewing the system for about 190 seconds. During this time, 105 total flashes (sum of cloud-to-cloud and intracloud) were observed in at least 6 convective cells, spanning an area of about 50,000 km^2. A coherent set of trajectories starting inside the NO plume crossed this area with enhanced lighting activity between 28 and 32° W / 43.5 to 46° N at about the time

when the lighting took place (Figure 15b). Using 70 % to 55 % as a preliminary estimate of OTD detection efficiency [*Boccippio et al.*, 1999], we estimate that the six cells had total flash rates of (1-2), (1-2), (2-2), (5-7), (11-15) and (24-30) flashes per minute, respectively. The latter rate indicates a significantly electrified deep convective storm. After 1300 UTC 970813, the cluster weakened considerably. Lightning was not anymore observed during the OTD overpasses at 0400 and 0700 UTC 970814.

Examination of the spatial agreement of successive OTD-observed background scenes suggests that the location errors for these flashes were no greater than 100 km, which should not significantly impact the current results.

The system described above thus developed deep convection for a relatively brief period (0300-1300 UTC 13 August) and was producing lightning at least from 0442-0932 UTC. At 0932, at least one cell in the system was producing lightning at a significant rate (24-30 flashes/minute).

We showed in the previous paragraphs that at the time of the claimed NO fixation in the thunderstorm, the background NO_x concentration was not particularly high and most probably fairly uniform since there are no indications of processes other than thunderstorms which could have significantly contributed to the observed high NO concentrations. Nevertheless did the observed NO_x concentrations exhibit two distinct local minima during the plume encounter. While we could find different flow regimes of the trajectories starting on the flight leg before the plume was observed and the one inside the plume, we could not make an equivalent observation for trajectories starting on the flight sections were the local minima were observed. The brightness temperature tracing and the animations could not either give any indication of the

nature for these differences in the measured concentrations. Due to this issue and because of the spotty temporal availability of data about the lighting activity in the area of interest, NO production rates per flash would be very difficult to estimate and would require a detailed model of a thunderstorm such as has been done by *Pickering et al.* [1998]. We conclude that the large concentration variations observed downwind of several convective systems reflect a state of the atmosphere where mixing processes have not yet evened out local concentration gradients which are most probably due to inhomogeneous exposure to lighting activity and small scale mixing processes. Sub-grid scale turbulent mixing processes are an important aspect which needs to be addressed in studies aiming at modeling the atmospheric NO_x concentrations downwind of convective systems.

3.4 Overview of the NO_x concentrations measured during POLINAT 2 and SONEX

The composite of all tropospheric NO_x measurements performed at cruising altitude (defined as the altitude range between 190-300 hPa) between August 13 and November 23, 1997 (Figure 17a) shows two marked concentration maxima: In August the plumes were found over the continent whereas between September and November, they were typically sampled over the sea – a few hundred kilometers off the coast. The stratospheric measurements (Figure 17b) exhibited much lower values, most probably because the large tropospheric NO_x^* plumes only rarely penetrated the tropopause (defined here as 2 PVU). However, on a few occasions, concentrations of up to 700 pptv could be observed in the stratosphere. It is not sure whether convective injection of pollutants really crossed the tropopause or whether the ECMWF model did not

properly resolve the tropopause altitude in these rare cases. Another, although less likely explanation for the large stratospheric concentrations might be that stratospheric flashes above the thunderstorms [*Boeck et al.*, 1995] caused NO_x production.

In the years 1995 and 1997, the mean NO_x concentrations at cruising altitude (190-300 hPa) between September and November were very similar and ranged from 100 to 150 pptv over the North Atlantic [40-60° N and 10-40° W] and between 190 and 280 pptv above the U.S. continent [30-60° N and 60-90° W]. (An overview with all horizontal and vertical NO_x and O_3 profiles can be found in *Jeker et al.* [1998]). The vertical NO_x^* profile over the U.S. continent (and the corresponding coast) (Figure 18b) shows a distinct maximum (300 pptv) below the tropopause with a considerably lower median value. Such an observation can not be made for the North Atlantic (Figure 18a). This difference can most probably be explained by the weaker convective events and accompanied lightning activity over the North Atlantic, as it is suggested from an OTD lightning climatology [*Christian and Latham,* 1998]. In mid-latitudes the tropopause acts as a barrier for vertical transport of pollutants and lightning produced NO_x into the stratosphere so that the resulting plumes spread out and cover large areas even though single convective events are of much smaller size. This observation is in agreement with simulated vertical profiles of lightning NO_x mass [*Pickering et al.* 1998]. The "patchy" occurrence of extended NO_x^* plumes below the tropopause leads to a log-normal probability density function of the tropospheric NO_x concentrations [*Brunner,* 1998]. Since the plumes are mostly constrained to the troposphere, the corresponding probability density function is much wider than in the stratosphere. As to be

expected, the tropospheric NO_x plumes lead to a much wider probability density function over the continent (Figure 19b) than over the Atlantic (Figure 19a).

4. Conclusion:

On the flights performed within the POLINAT-2 framework, we made automated measurements of NO_x and ozone in the North Atlantic Flight Corridor with the NOXAR instrumentation. The concentration range was similar to that reported from the first campaign [*Brunner,* 1998] and confirmed the patchy occurrence of large scale NO_x plumes close to the tropopause which lead to a log-normal NO_x probability density function [*Brunner et al.,* 1998].

In three case-studies we examined the origins of such plumes by combining back-trajectories with brightness temperature enhanced (IR) satellite imagery, with lightning observations from the U.S. National Lightning Detection Network (NLDN) and with observations from the Optical Transient Detector (OTD) satellite. In the first case of a pronounced frontal system over the North American continent, maps of convective influence explained well the locations of plume observations made on several consecutive days. In the second case, a NO_x plume was observed downwind of a cluster of marine thunderstorms associated with moderate U.S. east coast cyclogenesis taking place in early November. The short lifetime of NO_x at sea level excludes advected polluted air masses from the U.S. continent as a source for the observed NO_x plume. We show that the number of lightning flashes during the most recent convective encounter of the air masses is proportional to the NO_x concentrations observed several hundred kilometers downwind of the outflow of these thunderstorms. This leads to the conclusion that lightning discharges are

the dominant source of this NO_x plume. From the fact that the NO_x maximum in autumn and winter (during the first campaign) was found several hundred kilometers off the U.S. east coast, it can be inferred that thunderstorms triggered by the large temperature difference between the cold continental and the warm Gulf Stream surface temperatures, are important sources for the regional upper tropospheric NO_x budget during the cold seasons.

In the third case-study we describe an extended NO plume observed downwind of marine thunderstorms taking place in August. A constellation of several satellites made observations of deep convection in the North Eastern Atlantic – an area crossed by the back-trajectories originating in the plume. In addition, the OTD satellite reported strong lightning activity in the area of interest during several orbits. Since the air was trapped in a cut-off low and therefore isolated from anthropogenic influence for the previous four to five days, we conclude that this plume can also be attributed to lightning discharges. According to a lightning climatology obtained by the OTD satellite [*Christian and Lantham* 1998] the location of the strong lightning activity was rather untypical for the month of August. In this area lightning activity is more typical during winter months. Since marine lightning seems to produce large NO_x enhancements, it might explain the relatively large number of NO_x plumes found over the Atlantic in winter [*Brunner et al.*, 1998].

Interestingly, the concentration range of our NO_x plume observations, which we typically detected a few hundred kilometers downwind of the thunderstorms, is very similar to that reported in the literature on several anvil penetration missions [*Huntrieser et al.*, 1999]. Selected cases of the large number of observed NO_x plumes during NOXAR 1995/96 and POLINAT 2

might eventually be used to get better estimates about the relative importance of the lightning component to the NO_x budget along air routes.

Acknowledgements

The realization of this project would not have been possible without the help of all the parties mentioned below to whom we would like to express our gratitude: Swissair for installing and transporting the NOXAR instrumentation package and to Swissair Flight Dispatch for communicating the flight tracks to the DLR and SONEX project offices for the coordinated flights. To Hans Schlager (DLR) and Jim Eilers (NASA Ames) for handling the communication with Swissair and thus making the intercomparison flights possible. To Helmut Ziereis (DLR) for the NO bottle exchange allowing to establish a common gas standard. To Steve A. Goodman (NASA MSFC) for providing us with the National Lightning Detection Network Data. To Marion Legg (NASA Ames) for preparing the large amount of brightness temperature enhanced GOES-8 images. To Lyatt Jaglé, Harvard University, for the calculation of the NO_x residence time in the August marine convection case. To Olaf Morgenstern, Cambridge University, for the algorithm to calculate CAPE from ECMWF fields. To Eco Physics (Dürnten, Switzerland) for providing us with support during the campaign.

References:

Allen, D. J., K. E. Pickering, G. L. Stenchikov, A. M. Thompson, Y. Kondo, and L. Pfister, A 3-D NO_y simulation during SONEX using a stretched-grid chemical transport model, *to be submitted to J. Geophys. Res.*.

Baughcum, S. L., D. M. Chan, S. M. Happenny, S. C. Henderson, P. S. Hertel, T. Higman, D. R. Maggiora, and C. A. Oncina, Emissions scenarios development: scheduled 1990 and projected 2015 subsonic, Mach 2.0 and Mach 2.4 aircraft. In *The Atmospheric Effects of Stratospheric Aircraft: A Third Program Report* (edited by Stolarski R.S. and Wesoky H. L.) NASA Reference publication 1313, 1993.

Bethan, S., G. Vaughan, C. Gerbig, A. Volz-Thomas, and Richer H, and D.A. Tiddeman, Chemical air mass differences near fronts, *J. Geophys. Res.*, **103** 13413-13434, 1998.

Biazar, A.P., and R.T. McNider, Regional estimates of lightning production of nitrogen oxides, *J. Geophys. Res.*, **100**, 22861-22874,1995.

Boeck ,W. L., O.H Vaughan., R.J. Blakeslee, B. Vonnegut, M. Brook, and J. McKune, Observations of lightning in the stratosphere, *J. Geophys. Res.*, **100**,1465-1475,1995.

Boccippio, D.J., K. Driscoll, W. Koshak, R. Blakeslee, W. Boeck, D. Mach, H.J. Christian, and S. J. Goodman, Cross-sensor validation of the Optical Transient Detector (OTD), *Journal-of-Atmospheric-and-Solar-Terrestrial-Physics*, **60**, 701-712, 1998.

Brunner, D., One Year Climatology of Nitrogen Oxides and Ozone in the Tropopause Region (Results from B-747 Aircraft Measurements), *Diss. ETH Nr. 12556*, 1998.

Brunner D., J. Staehelin, and D. Jeker, Large-scale Nitrogen Oxide Plumes in the Tropopause Region and Implications for Ozone, *Science*, **282**, 1305-1309, 1998.

Chatfield R. B. , P. J. Crutzen, Sulfur-Dioxide in Remote Oceanic Air – Cloud transport of reactive precursors, *J. Geophys. Res.*, **89**, 7111-7132, 1984.

Christian, H.J, K.T. Driscoll, S.J. Goodman, R.J. Blakeslee, D.A. Mach, and D.E. Buechler, The Optical Transient Detector (OTD), Proc. 10th International Conference on Atmos. Electricity, ICAE, Osaka, Japan, 1996.

Christian, H. J., Latham J., Satellite measurements of global lightning, *Q. J. R. Meteorol. Soc.*, **124**, 1771-1773 Part A,1998.

Cramer, J.A., and K. L. Cummins, Long Range And Trans-oceanic Lightning Detection, Proceedings International Lightning Detection Conference, Tucson AZ, November 1998.

Cummins, K.L., M. J. Murphy, E. A. Bardo, W. L. Hiscox, R. B. Pyle, and A. E. Pifer, A combined TOA/MDF Technology Upgrade of the U.S. National Lightning Detection Network, *J. Geophys. Res*, **103**, 9035-9044, 1998.

Dias-Lalcaca, P., D. Brunner, W. Imfeld, W. Moser, and J. Staehelin, An automated system for the measurement of nitrogen oxides and ozone concentrations from a passenger aircraft-instrumentation and first results of the NOXAR project, *Environ. Sci. Technol.*, **32**, 3228, 1998.

Dickerson, R. R. , G. J. Huffman, W. T. Luke, L. J. Nunnermacker, K. E. Pickering, A. C. D. Leslie, C. G. Lindsey, W. G. N. Slinn, T. J. Kelly, P. H. Daum, A. C. Delany, J. P. Greenberg, P. R. Zimmerman, J. F. Boatman, J. D. Ray, and D. H. Stedman, Thunderstorms: An important mechanism in the transport of air pollutants, *Science*, **235**, 460-464, 1987.

Ehalt, D. H., and F. Rohrer, The impact of commercial aircraft on tropospheric ozone. In the Chemistry Atmosphere – Oxidants and Oxidation in the Earth's Atmosphere. 7th BOC Priestley Conference, Lewisburg, Pennsylvania, 1994 (edited by Brandy A. R.) pp. 105-120, The Royal Society of Chemistry, Special Publication No. 170, 1995.

Fishman, J., S. Solomon, and P. J. Crutzen, Observational and theoretical evidence in support of a significant in-situ photochemical source of tropospheric ozone, *Tellus*, **31**, 432-446, 1987.

Franzblau, E., C. J. Popp, Nitrogen-Oxides Produced from Lightning, *J. Geophys. Res.*, 94, 11089-11104, 1989.

Gardner et al., submitted to xx

Goldenbaum, G. C., and R. R. Dickerson, Nitric-Oxide Production by Lightning Discharges, *J. Geophys. Res*, **98**, 18333-18338, 1993.

Helas, G. and, P. Warneck, Background NO_x mixing ratios in air masses over the North Atlantic Ocean, *J. Geophys. Res.*, **86**, 7283-7290, 1981.

Höller, H., U. Finke, H. Huntrieser, M. Hagen, and C. Feigl, 1999, Lightning produced NO_x (LINOX) - Experimental design and case study results, *J. Geophys. Res., in press.*

Huntrieser, H., H. Schlager, C. Feigl, and H. Höller, Transport and production of NO_x in electrified thunderstorms: Survey of previous studies and new observations at midlatitudes, *J. Geophys. Res.*, **103**, 28,247-28,264, 1998.

Idone, V.P., D. A. Davis, P. K. Moore, Y. Wang, R. W. Henderson, M. Ries, and P. F. Jamason, Performance evaluation of the U.S. National Lightning Detection Network in eastern New York. 2. Location accuracy, *J. Geophys. Res.*, **103**, 9057-9069, 1998.

Idone, V. P., A. B. Saljoughy, R. W. Henderson, P. K. Moore, and R. B. Pyle, A reexamination of the peak current calibration of the National Lightning Detection Network, *J. Geophys. Res.*, **98**, 18323-18332, 1993.

Jaeglé, L., D. J. Jacob, Y. Wang, A. J. Weinheimer, B. A. Ridley, T. L. Campos, G. W. Sachse, and D. E. Hagen, Sources and chemistry of NO_x in the upper troposphere over the United States, *Geophysical-Research-Letters*, **25**, 1705-1708, 1998.

Jeker, D., J. Staehelin, and D. Brunner, Nitrogen Oxides and Ozone from B-747 measurements (August to November 1997). In *POLINAT 2 report* (Schumann, 1999), p. 31 ff., 1999.

Lacis, A.A., D. J. Wuebbles, and J. A. Logan, Radiative forcing of climate by changes in the vertical distribution of ozone, *J. Geophys. Res.*, **95**, 9971-9981, 1990.

Lee D. S., I. Köhler, E. Grobler, F. Rohrer, R. Sausen, L. Gallardo-Klenner, J. J. G. Olivier, F. J. Dentener, and A. F. Bouwman, Estimates of global NO_x emissions and their uncertainties, *Atmos. Environ.*, **31**, 1735-1749, 1997.

Luke, W.T., R. R. Dickerson R.R., W. F. Ryan, K. E. Pickering, L. J. Nunnermacker,Tropospheric Chemistry over the lower Great-Plains of the United-States. 2. Trace Gas Profiles and Distributions, *J. Geophys. Res.*, **97**, 20647-20670, 1992.

Meyer, C. P, C. M. Elsworth, and I. E. Galbally, Water vapor interference in the measurement of ozone in ambient air by ultraviolet absorption, *Rev. Sci. Instrum.* **62(1)**,

223-228, 1991.

Murphy, D. M., D. W. Fahey, M. H. Proffitt, S. C. Liu, K. R. Chan, C. S. Eubank, S. R. Kawa, and K. Kelly, Reactive nitrogen and its correlation with ozone in the lower stratosphere and upper troposphere, *J. Geophys. Res.*, **98**, 8751-8773, 1993.

Orville, R. E., Winter lightning along the East Coast, Geophys. Res. Lett., 17, 713-715, 1990.

Pickering, K. E., A. M. Thompson, L. Pfister, T. L. Kucsera, Y. Kondo, G. W. Sachse, B. E. Anderson, and D. R. Blake, Comparison and interpretation of chemical measurements from two SONEX flights over the Canadian maritimes: Lightning, convection and aircraft signatures, *to be submitted to J. Geophys. Res.*

Pickering, K., W. Yansen, W. K. Tao, C. Price, and J. F. Muller, 1998: Vertical Distributions of Lightning NO_x for use in regional and global chemical transport models, *J. Geophys. Res.*, **103**, 31203-31216, 1998.

Poulida, O., and R. R. Dickerson, A. Heymsfield, Stratosphere-troposphere exchange in a midlatitude mesoscale convective complex. 1. Observations *J. Geophys. Res.*, **101**, 6823-6836, 1996.

Ryall, D.B., R. H. Maryon, R. G. Derwent, and P. G. Simmonds, Modelling long-range transport of CFCs to Mace Head, Ireland, *Q. J. R. Meteorol. Soc.*, **124**, 417-446, 1998.

Selkirk, H. B., J. Hannan, G. Bieberbach, L. Pfister, A. M. Thompson, G. L. Gregory, G. W. Sachse, and Y. Kondo, An intercomparison of isentropic and kinematic back trajectories from tropopaU.S.e folding events over the North Atlantic region, *to be submitted to J. Geophys. Res.*

Schiff, H.I., D. Pepper, and B. A.Ridley, Tropospheric NO measurements up to 7 km *J. Geophys. Res.*, **84**, 7895-7897, 1979.

Ridley, B. A., J. E. Dye, J. G. Walega, J. Zheng, F. E. Grahek, and W. Rison, On the production of active nitrogen by thunderstorms over New Mexico, *J. Geophys. Res.*, **101**, 20985-21005, 1996.

Schlager, H., P. Schulte, H. Ziereis, and U. Schumann, 1996, Airborne observations of large scale accumulations of air traffic emissions in the North Atlantic flight corridor within a stagnant anticyclone, *Proceedings of the International Colloquium on Impact of Aircraft Emissions Upon the Atmosphere, Paris 15-18 October 1996, p.247-252. ONERA*

Schlager, H., P. Konopka, P. Schulte, U. Schumann, H. Ziereis, F. Arnold, M. Klemm, D. E. Hagen, P. D. Whitefield, and J. Ovarlez, In situ observations of air traffic emission signatures in the North Atlantic flight corridor, *J. Geophys. Res.*, **102**,10739-10750, 1997.

Schumann, U. (ed), The impact of nitrogen oxide emissions from aircraft upon the atmosphere at flight altitudes-Results from the AERONOX project, *Atmospheric Environment*, **21**, 1723-1733, 1997.

Schumann, U., H. Schlager, F. Arnold, J. Ovarlez, H. Kelder , Ø. Hov, G. Hayman, I. S.A. Isaksen, J. Staehelin, and P. D. Whitefield, Pollution from aircraft emissions in the North Atlantic flight corridor: Overview on the POLINAT project, *J. Geophys. Res. (this issue)*

Stohl, A., and P. Seibert, Accuracy of trajectories as determined from the conservation of meteorological tracers, *Q. J. R. Meteorol. Soc.*, **124**, 1465-1484, 1998.

Thompson, A.M., Sparling L.C., Y. Kondo, B.E Anderson., G. L. Gregory, and G. W. Sachse, Fingerprinting NO_x on SONEX: What was the aircraft contribution to NO_x and NO_y?, *submitted to Geophyical Research Letters (special section on POLINAT 2 / SONEX).*

Thompson, A. M., L. Pfister, T. L. Kucsera, L. R. Lait, H. B. Selkirk, K. E. Pickering, Y. Kondo, and G. Gregory, The Goddard/Ames Meteorological Support and Modeling System during SONEX: Evaluation of analyses and trajectory-based model products with tracer data, *to be submitted to J. Geophys. Res.*.

von Liebig, J ., Une note sur la nitrification, *Ann. Chem. Phys.*, **35**, 329-333, 1827.

Wacker, R.S., and Orville R.E., Changes in measured lightning flash count and return stroke peak current after the 1994 U.S. National Lightning Detection Network upgrade. 1. Observations, *J. Geophys. Res.*, **104**, 2151-2157, 1999.

Wennberg, P. O., T. F. Hanisco, L. Jaeglé, D. J. Jacob, E. J. Hintsa, E. J. Lanzendorf, J. G. Anderson, R. S. Gao, E. R. Keim, S. G. Donnelly, L. A. Del Negro, D. W. Fahey, S. A. McKeen, R. J. Salawitch, C. R. Webster, R. D. May, R. L. Herman, M. H. Proffitt, J. J. Margitan, E. L. Atlas, S. M. Schauffler, F. Flocke, C. T. McElroy, and T. P. Bui, *Science*, **279**, 49-53, 1998.

Wernli, H., and Davies HC , A Lagrangian-based analysis of extratropical cyclones .1. The method and some applications, *Q. J. R. Meteorol. Soc.*, **123**, 467-489, 1997.

Witte J.C., I. A. Folkins, J. Neima, B. A. Ridley, J. G. Walega, and A. J. Weinheimer, Large-scale enhancements in NO/NO_y from subsonic aircraft emissions: comparisons with observations, *J. Geophys. Res.*, **102**, 28169-28175, 1997.

Zel'dovich, Y.B., and Y.P. Raiyer, Physics of Shock Waves and High Temperature Hydrodynamic Phenomena, 566-571, Academic, San Diego, Calif., 1967.

Ziereis, H., H. Schlager, and P. Schulte, NO, NO_y, and O_3 Intercomparisons during POLINAT 2, in *POLINAT 2 report* (Schumann, 1999), p. 55 ff., 1999.

Zipf, E. C., and S. S. Prasad, Evidence for new sources of NO_x in the lower atmosphere, *Science*, **279**, 211-213, 1998.

Figure captions

Figure 1a-c. Scatter plot of the ECMWF fields interpolated in space and time along the flight track versus the meteorological measurements (2 minute averages) made with the B-747 standard sensors. All flights between Zurich and the United States which were performed between August 13 and November 23, 1997 are considered. The East wind component (a) was on average about 30 m/s (considering both west-and eastbound flights) whereas the North wind component (b) has an average of about 0 m/s. As to be expected the largest scatter in the temperatures (c) occurred close to the tropopause where average temperatures of about –50° C were measured.

Figure 2. Estimated aircraft NO influence along the flight track. The three lines indicate 5d, (lower thin gray line) 10d (bold line), and eternal (upper thin gray line) 1/e NO_x lifetimes. There

is a strong increase of the aircraft attributable NO_x on the westbound approach of the U.S. east coast on November 9, 1997. Note also the large variation of the estimated aircraft influence even on neighboring flight legs.

Figure 3 a-b. Formation of a weak surface cyclone at the U.S. east coast on September 11 (Figure 3a). The thin lines indicate the 900 hPa potential temperature contours (contour interval 2 K). The bold lines symbolize the 900 hPa geopotential height (contour interval 30 m). The shaded area in Figure 3a indicates the region where the potential vorticity (PV) exceeds 2 PVU on the 335 K isentropic surface. In Figure 3b the thick line indicates the location the intersection of the 2 PVU level with the 335 K isentropic surface and the shaded area indicates high CAPE (Convective Available Potential Energy) levels over the coast.

Figures 4 a-c. Time series plots of the NOXAR westbound NO measurements (3 sec. averages) performed between September 11 and 13, 1997 (upper graphs) and maps of convective influence for cruising altitude (lower graphs) of the respective days. The flight track in the maps is plotted in white color. Black areas indicate that no convective event occurred during the previous five days. Colored grid cells indicate the time since most recent convection.

Figure 5. Box plot comparing NO samples with (left part in graph) and without (right part) a convective encounter during the previous 5 days as determined from the maps of convective influence. For the boxes which are marked with „No AC" we subtracted both the short spikes and

the values that we obtained from an ANCAT tracing from the NO measurements (assuming a NO_x residence time of 10 days). For the boxes marked with „AC" we used all measurements (without performing an aircraft influence filtering in the above sense). The horizontal white line indicates the median values, the notches the confidence interval of the medians. Thin horizontal lines indicate isolated measurements.

Figure 6a. Tracks (bold lines) of the SONEX (full line) and NOXAR (dashed lines) flights of November 9/10, 1997. Kinematic ECMWF back trajectories starting along the flight tracks are represented with thin lines. NO concentrations in excess of 1000 pptv are symbolized with black squares. Note the different motion of the trajectories originating on a flight leg with low NO_x concentrations (upper dashed track) in section 3 and the back trajectories starting in the NO_x plumes observed by SONEX (section 2), by NOXAR westbound (section 1) and NOXAR eastbound (below section 3) which followed an upper-level trough associated with a low pressure system. The trajectories belonging to the second sub plume (thick dashed lines) of the NOXAR westbound flight crossed an area where the National Lightning Detection Network (long range channel) reported strong lighting activity (contour plots for period of 2100 to 2300 UTC on November 8). The locations of these trajectories during this time interval are highlighted with black markers on the trajectories. Section C marks an area where the convective clouds reached the altitudes of the overpassing trajectories, B the warm Gulf Stream and A the comparatively cold continent.

Figure 6b. Vertical flight profiles of SONEX flight 14 (grey full line) and NOXAR flight 762 west- and eastbound (gray dashed lines). The flight direction of the NOXAR flights is indicated by arrows. Flight legs with NO concentration (NO_2 on NOXAR eastbound) greater than 1000 pptv are marked with black dots. The numbers indicate flight sections of interest: 1 denotes the flight leg on which during NOXAR westbound NO_x concentrations in excess of 3000 pptv NO were detected, 2 marks the SONEX cross-corridor flight leg. In section 3 low NO levels were sampled on the NOXAR westbound but high levels of NO_2 on NOXAR eastbound flight.

Figure 7a. Elongated zone of strong baroclinicity between Florida and the central Atlantic on November 7 at 1200 UTC. The symbols are the same as in Figure 3.

Figure 7b. Same as Figure 7a but for 12 UTC November 9, 1997. The track of the NOXAR B-747 westbound is symbolized with "O" in areas where the NO concentrations were smaller than 1000 pptv and with "X" where the concentrations exceeded this level. The flight level corresponded approximately to the 327 K isentropic level.

Figure 8a. GOES-8 image from November 8, 1997 at 2145 UTC. The white rectangle encloses a band of high reaching convective clouds (black) which exhibited very strong lighting activity between November 8 at 2000 UTC and November 9 at 0500 UTC. The white boxes and triangles

are points from the back trajectories starting inside the NO plume and indicate the location of the respective air masses at the time of the satellite picture. Triangles symbolize air masses from the first sub-plume (< 1000 pptv) observed between 1400 and 1500 UTC and boxes symbolize air from the second sub plume (< 3000 pptv) observed between 1515 and 1545 UTC. (*High resolution imagery has been ordered to improve the quality of the graph for an eventual final version*).

Figure 8b. The line-dotted lines are the 80 and 90 % relative humidity contours at 900 hPa which form a T-bone frontal structure 1200 UTC on November 9, 1997. The dark areas show elevated CAPE values.

Figure 9. NO measurements from the SONEX DC-8 aircraft (thick, dark gray line) and the NOXAR B-747 westbound flight (thin black line) performed on November 9, 1997. The NOXAR NO concentration enhancement can be subdivided into three sub plumes marked with I to III. On the respective eastbound flight at night, the B-747 detected very elevated NO_2 concentrations (thin, light gray line) downwind of the area where SONEX detected the highly elevated NO and NO_y concentrations.

(Note: For the time being we used 1 min. averaged SONEX measurements and 3 s data for the NOXAR system. At revision time we would plot 3 sec. averaged data for both platforms).

Figure 10. Temperatures of the GOES-8 derived convective cloud tops (crosses) and temperatures of the ECMWF back trajectories (diamonds) starting inside first NOXAR sub-

plume at 1500 UTC on 971109. Three temperature regimes are clearly visible: In section A the trajectories are over the comparatively cold U.S. continent, in B over the warm Gulf Stream Current, in C they cross a region of intense convective activity reaching to the altitude of the overpassing trajectories.

Figures 11 a, b. Quantitative analysis of the lightning encounter on the NOXAR westbound flight on November 9, 1997. The upper panel (Figure 11a) indicates the maximum (bold line) and median value (thin line) of the number of lightning flashes encountered by the back trajectories during the most recent convective encounter (we averaged at steps of 0.75 deg. and therefore get several values so that different statistical measures can be indicated). The lower panel (Figure 11b) shows the averaged NO measurements (bold line) and the measurements minus the ANCAT estimated aircraft influence (thin dotted line).

Figure 12. 3.5 day ECMWF back trajectories started along a line at 70° W longitude at 800 hPa on November 9, 1997 at 0000 UTC. The stars separate 24 hour intervals along each trajectory. The two airmasses which come together at the cold front do not originate in the polluted U.S. planetary boundary layer.

Figure 13. The upper graph shows the aircraft altitude (thick line) and the altitude of the tropopause (the grey shaded area covers the altitude range with PV values between 2 and 4) along

the flight track. The lower graph shows the ozone (grey line) and the 3 second averages of the NO measurements (black area) from the August 14 flight between Zurich to Chicago.

Figure 14a. The upper PV level development leads to a cut-off formation at 0000 UTC on August 11. Same symbols as in Figure 3a.

Figure 14b. Same as Fig. 14a but for August 14 at 1200 UTC. The flight track is marked with circles and with "X" where the 2 minute averaged NO concentration exceeded 700 pptv.

Figure 15a. The back trajectories (blue) starting on the flight track with high NO concentrations crossed an area where the OTD sensor reported lightning activity (red) between 0930 and 0936 UTC on 970813. The location of the trajectories between 0800 and 1000 UTC are marked with green markers.

Figure 15b. Zoom into the situation of Figure 15a. Contours of the OTD lightning intensity. The ECMWF back trajectories starting on the flight leg with elevated NO concentrations cross the areas of the reported lighting activity. The thick line on the trajectories indicates the time between 0800 to 1000 UTC on August 13. (The grid lines are separated by 2 degrees).

Figure 16. Brightness tracing plot of the trajectories starting on the flight leg between 1115 and 1145 UTC on August 14 where high NO values were observed. Big diamonds indicate

trajectories where the trajectory temperature was equal or higher than the GOES-8 derived temperature of the underlying convective cloud (crosses). Small diamonds show trajectory points where no convective influence took place. It can be derived that about 26 hours prior to start of the trajectories marine convective clouds reached to the altitude of the trajectories.

Figures 17 a, b. Composite of all 2 minute averaged NO_x measurements performed at cruising altitude (300-190 hPa) in the period of August 13 to November 23, 1997. The tropospheric values (PV< 2PVU) exhibited significantly lower values than the stratospheric values (Figure 17b).

Figure 18 a,b. Vertical NO_x* profile, over the North Atlantic Flight Corridor (left) the U.S. east coast (right). The median values are connected with a line, the mean values are marked with squares. In the plots, the scatter is described by the difference between the 10 and the 90% quantiles and is symbolized with a horizontal line connecting them. The number of 2 min. averages available in each class is indicated at the right hand side of the plot. (Only data between 190-300 hPa have been considered.)

Figure 19 a,b. Histograms and log normal probability density distribution dn/dln(c) of all NO_x* measurements in the North Atlantic Flight Corridor (left) and over the U.S. East coast and the

continent (right). Also shown are log-normal fits. The thin line indicates the tropospheric and the thick line the stratospheric values.

Tables:

Run	35 N	45 N	55 N	65 N	75 N
Standard Run	3.8	4.1	4.6	5.6	10.9
Aerosol surface area (SA)=2	4.5	4.8	5.4	6.6	12.0
Pres=200, SA=9	4.4	4.7	5.3	6.5	11.8
Pres=400, SA=9	1.7	1.8	2.0	2.4	4.3

Table 1. Lifetimes (1/e) in days for NO_x between 35 and 75N. The following parameters have been used to initialize the model (standard run): T= 223 K @ p= 270 mbar and T=240K @ 400 mbar, O_3=100 ppbv, H_2O= 70 ppmv, CH_4= 1750 ppmv, CO= 70 ppbv, Surface_area (SA)= 9 $\mu m^2/cm^3$

Date	Time	Event
970812	0700	Reverse trajectory first enters GOES cloud cluster
	0800	OTD observes no lightning
	1015	OTD observes 15 flashes in up to 5 storms
	2200	GAI long range nighttime coverage begins
970813	0050	OTD observes 15 flashes in 2-4 storms
	0300	Cloud tops begin to rapidly deepen
	0442-0634	GAI observes 4 ground flashes at 04:42, 05:39, 06:33 06:34 UTC
		(40.4N/33.6W;45.2N/27.4W;44.4N,30.7W;45.2N,30.2W)
	0800	GAI long range nighttime coverage ends
	0800-1000	Period of GOES coldest cloud tops
	0900-1500	Period of DMSP coldest cloud tops
	0932	OTD observes 105 flashes in up to 6 storms
	1600	System weakens considerably (GOES)
	2200	GAI long range nighttime coverage begins
970814	0040	OTD observes no lightning
	0300	Reverse trajectory exits GOES-observed cloud cluster
	0700	OTD observes no lightning
	0800	GAI long range nighttime coverage ends
	1130	Aircraft observation of parcel

Table 2: Evidence of convective/lightning activity over the North Atlantic in the area of interest.

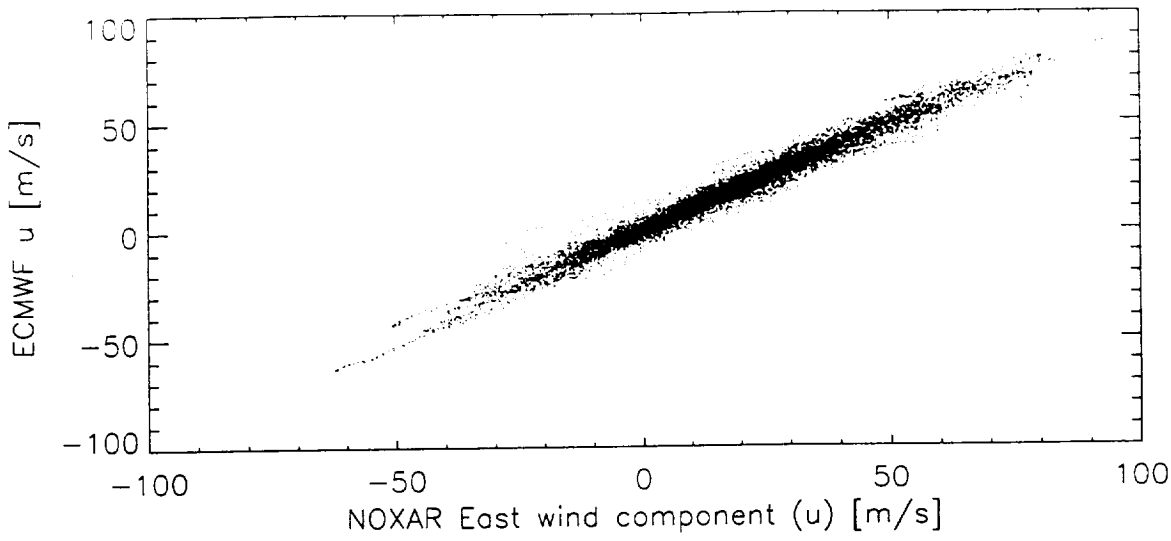
ECMWF u [m/s]
100
50
0
−50
−100
−100
−50
0
50
100
NOXAR East wind component (u) [m/s]

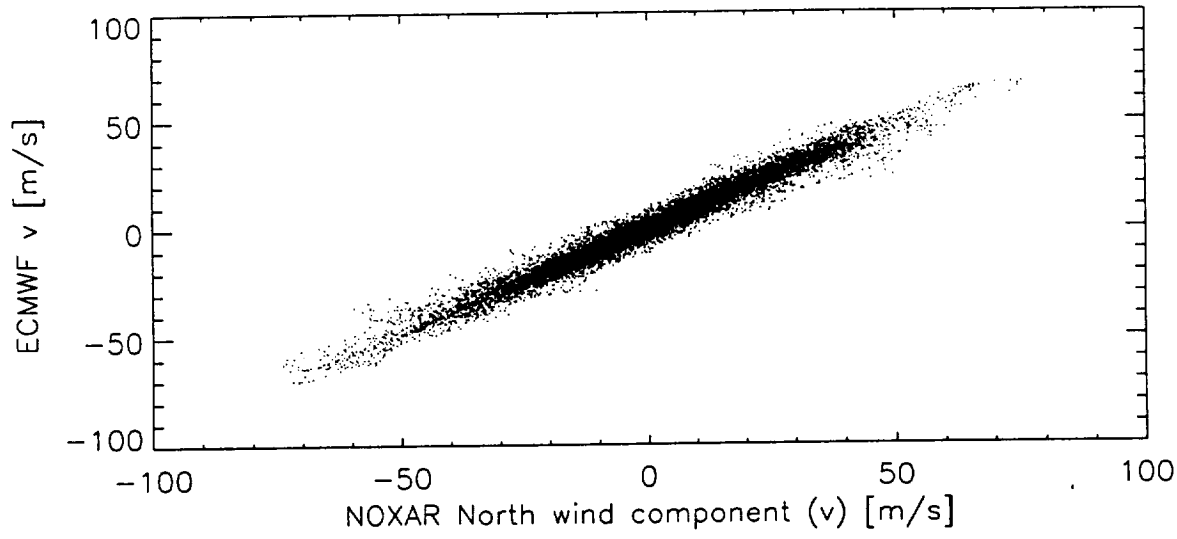
ECMWF v [m/s]
100
50
0
−50
−100
−100
−50
0
50
100
NOXAR North wind component (v) [m/s]

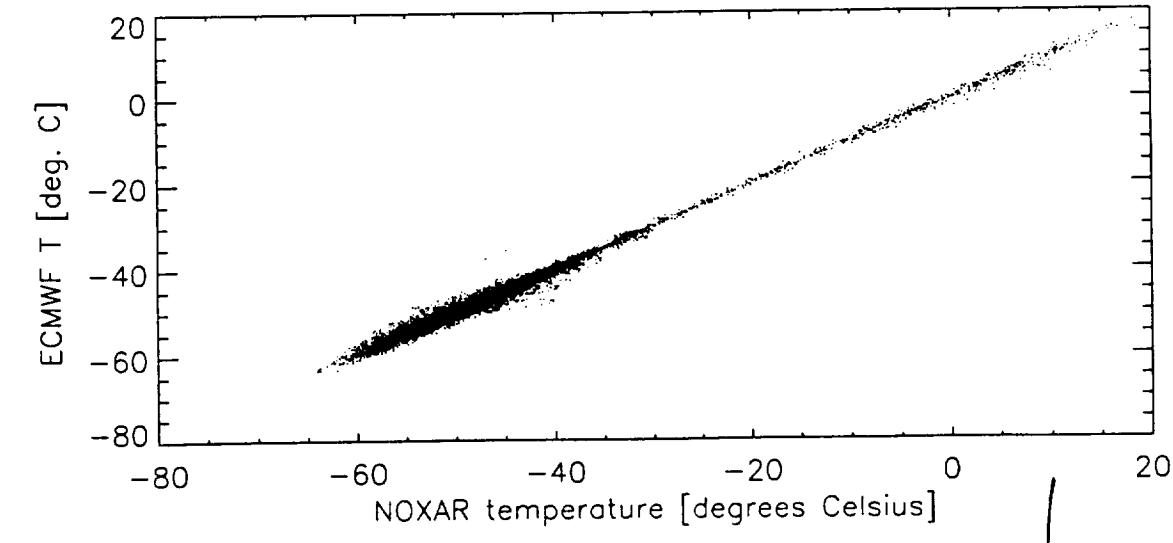
ECMWF T [deg. C]
20
0
−20
−40
−60
−80
−80
−60
−40
−20
0
20
NOXAR temperature [degrees Celsius]

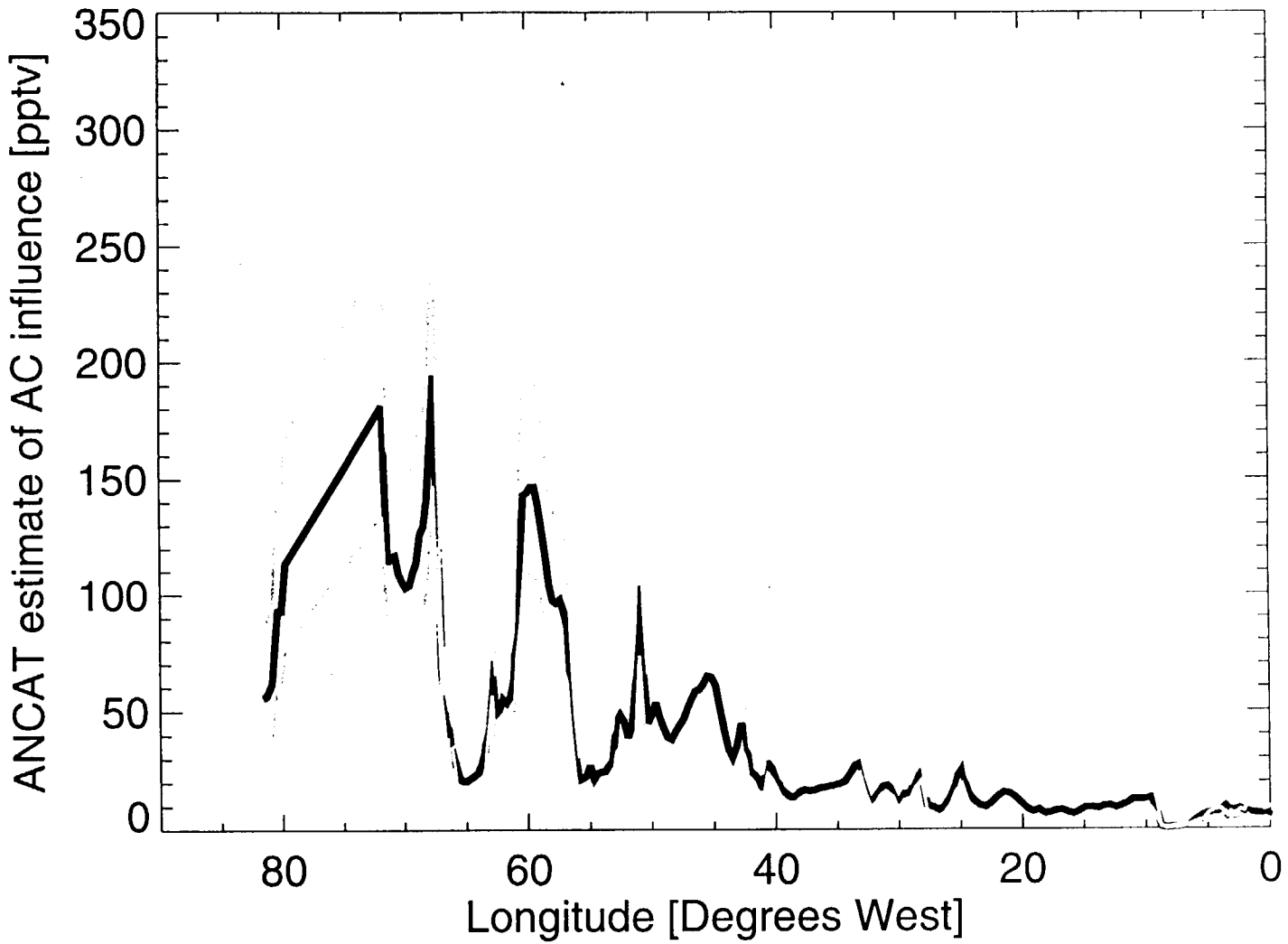
ANCAT estimate of AC influence [pptv]
350
300
250
200
150
100
50
0
80
60
40
20
0
Longitude [Degrees West]

2

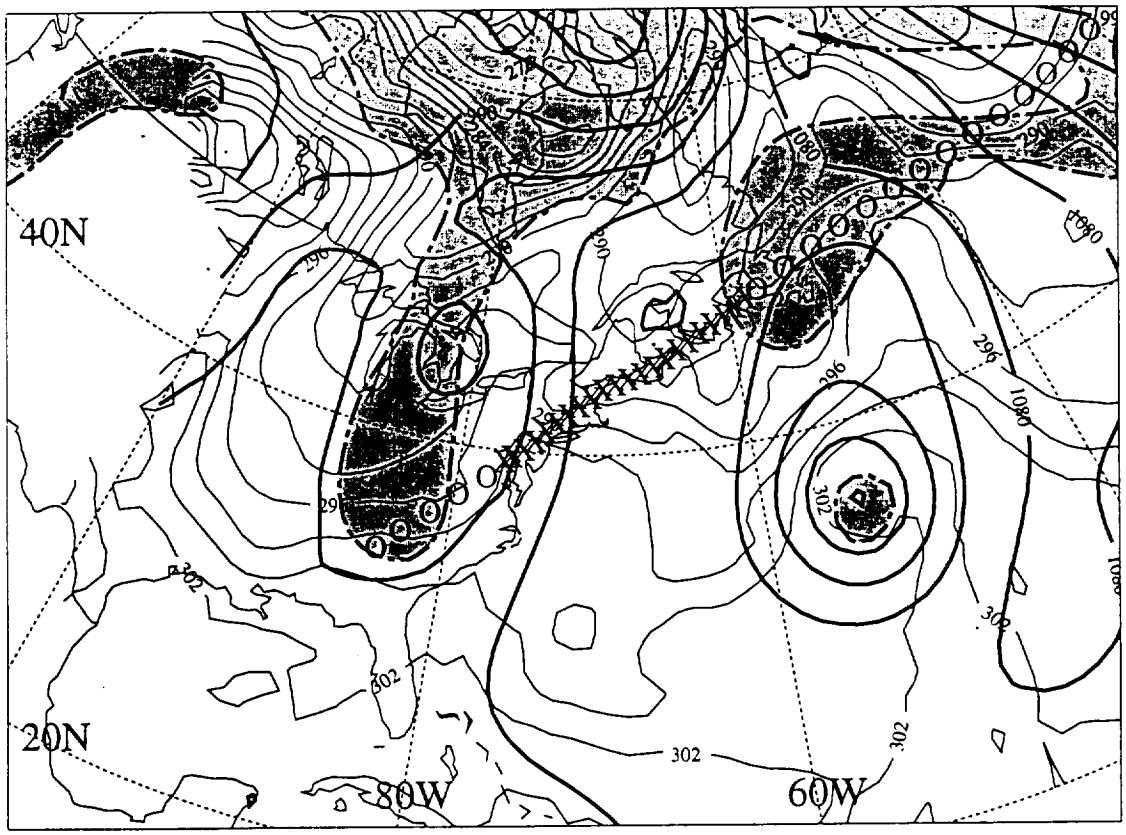

3a

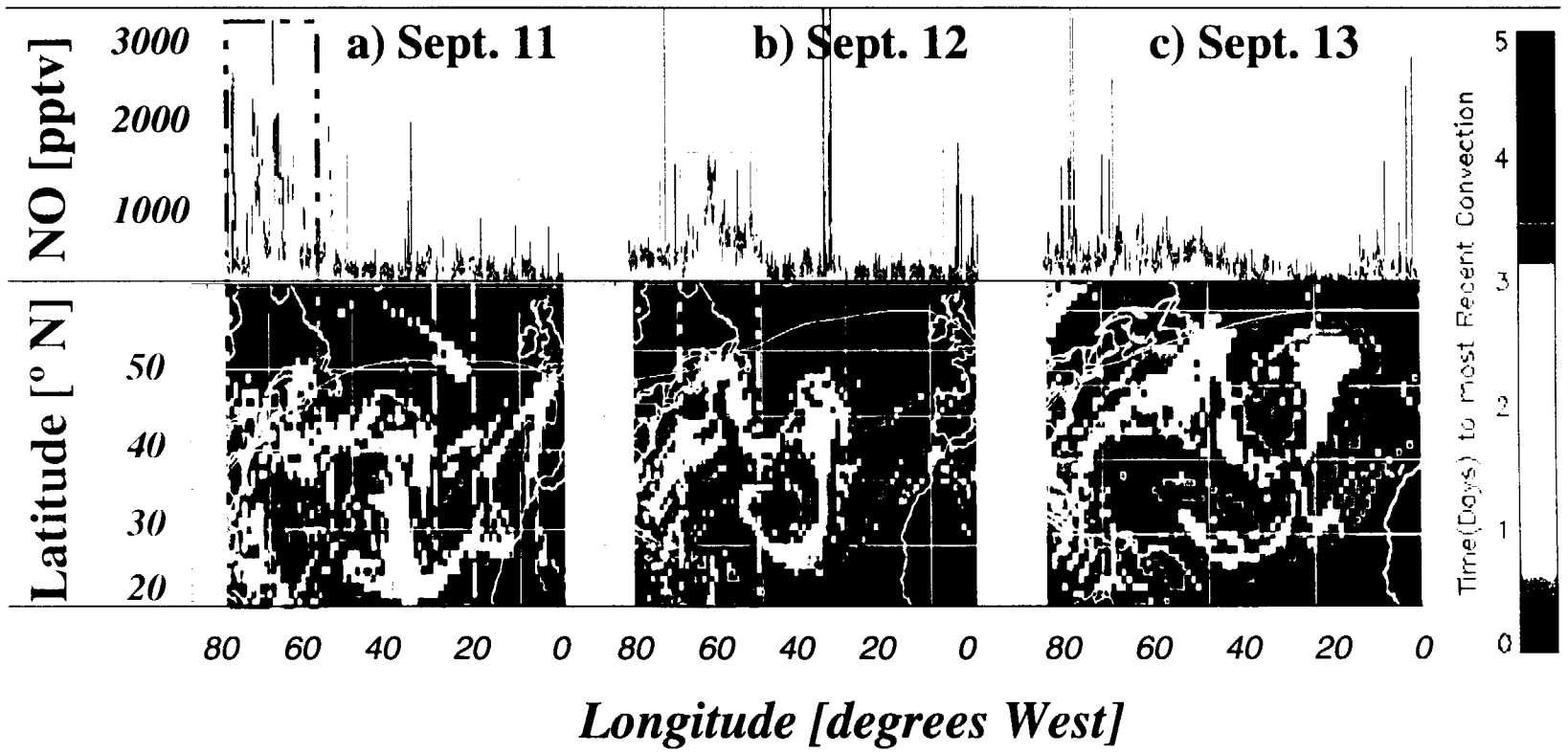
a) Sept. 11
b) Sept. 12
c) Sept. 13
NO [pptv]
3000
2000
1000
Latitude [° N]
50
40
30
20
80 60 40 20 0 80 60 40 20 0 80 60 40 20 0
Longitude [degrees West]
Time(Days) to most Recent Convection
5
4
3
2
1
0

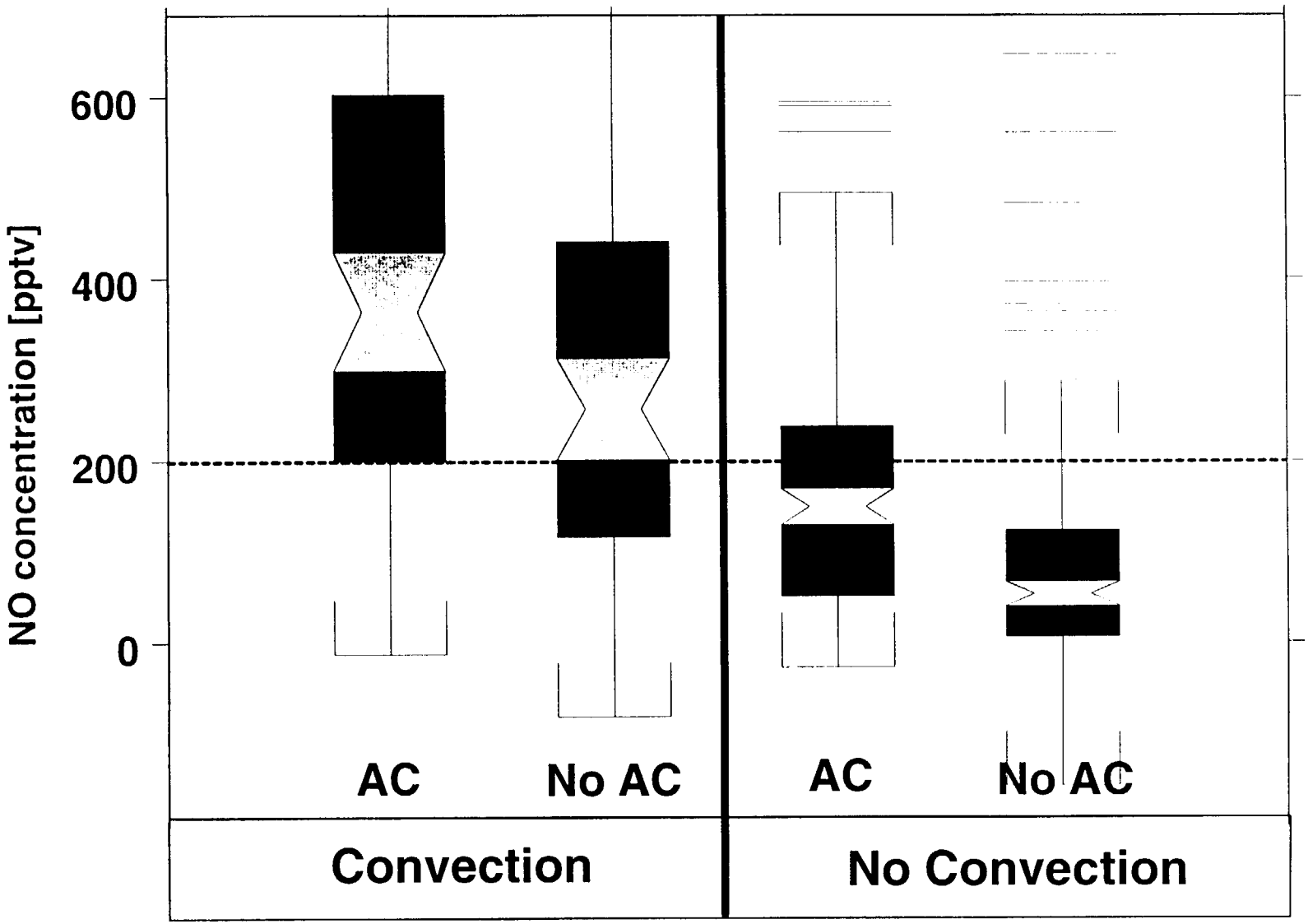
NO concentration [pptv]
600
400
200
0
AC
No AC
AC
No AC
Convection
No Convection

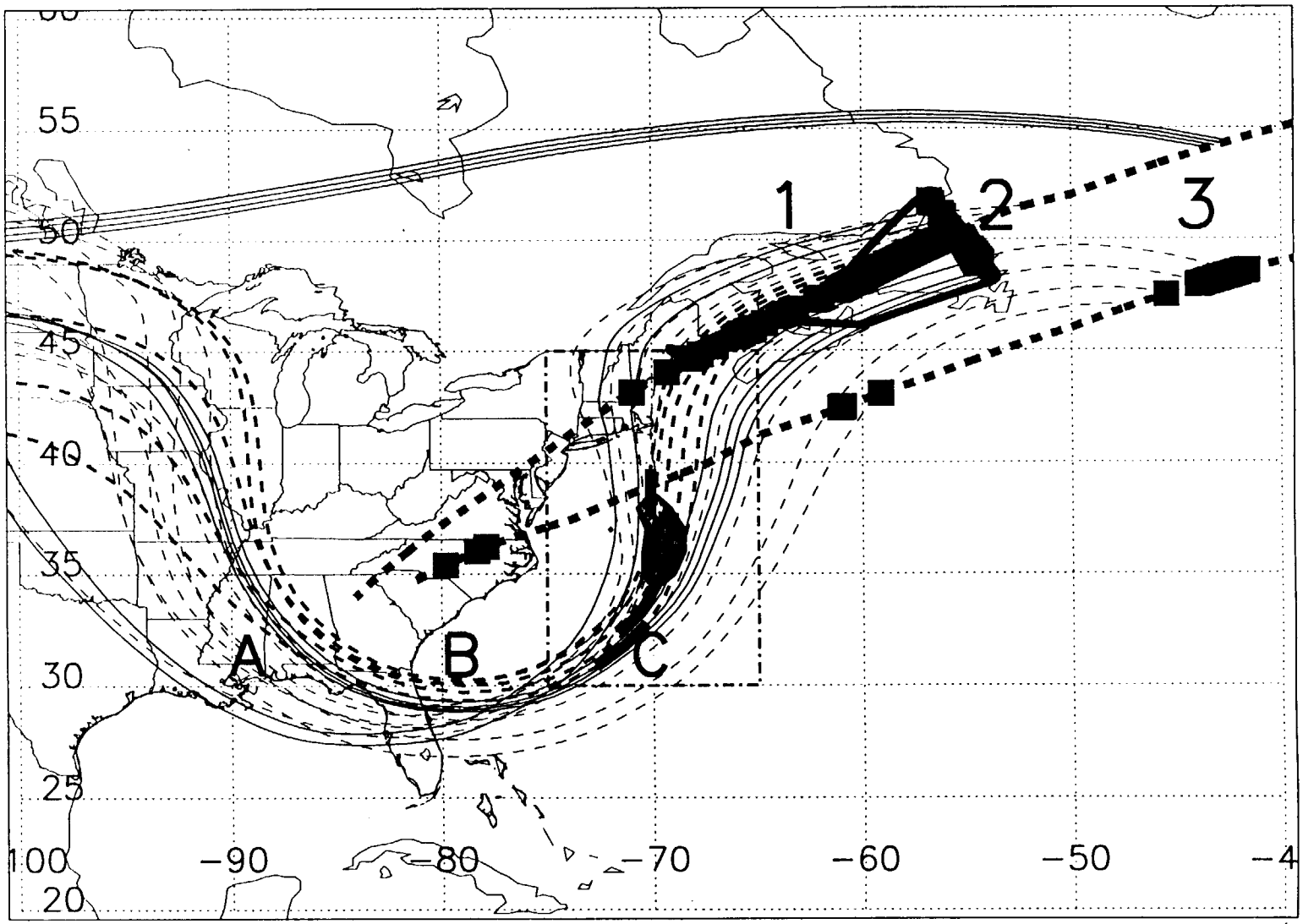

6d

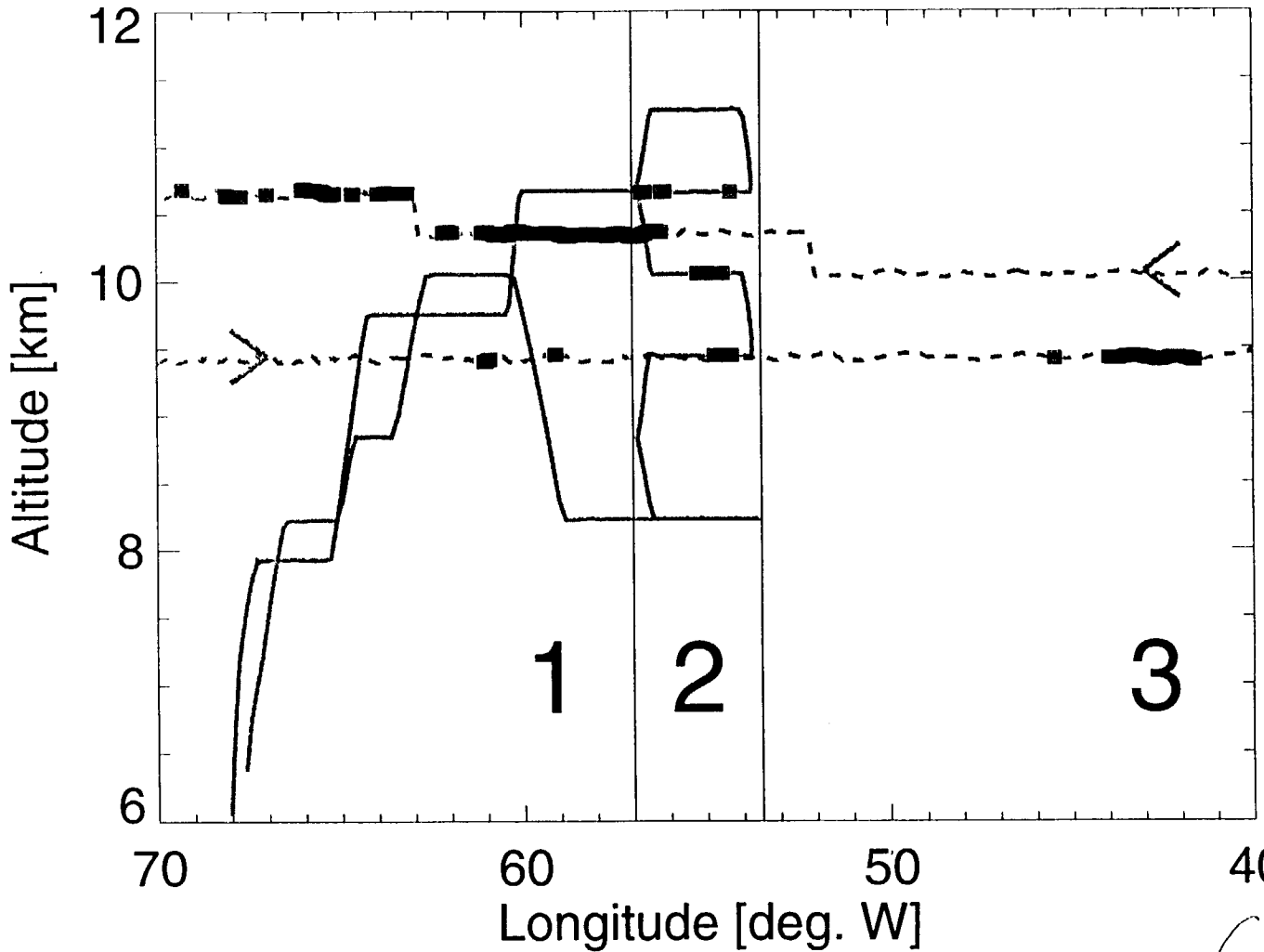

6b

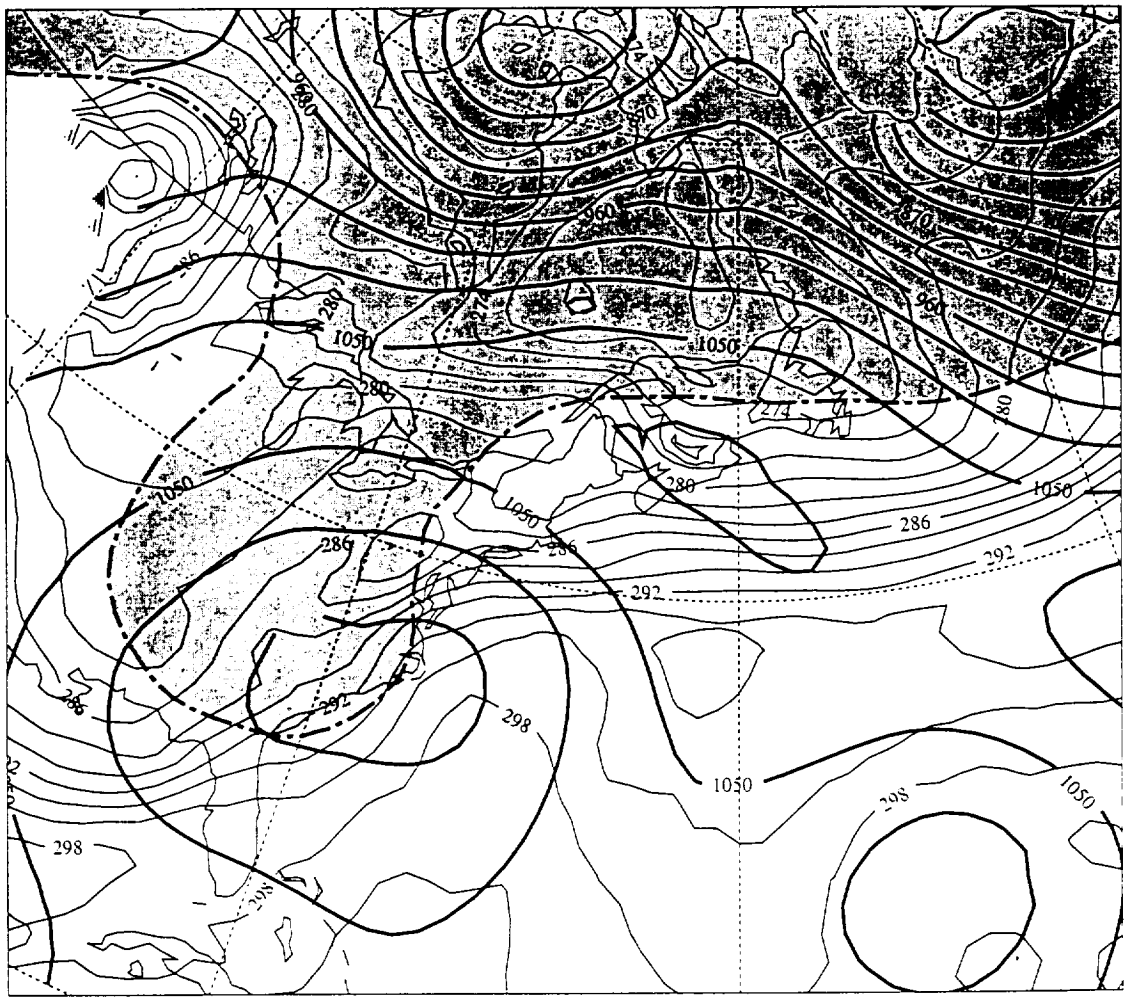
960
1050
280
286
292
298

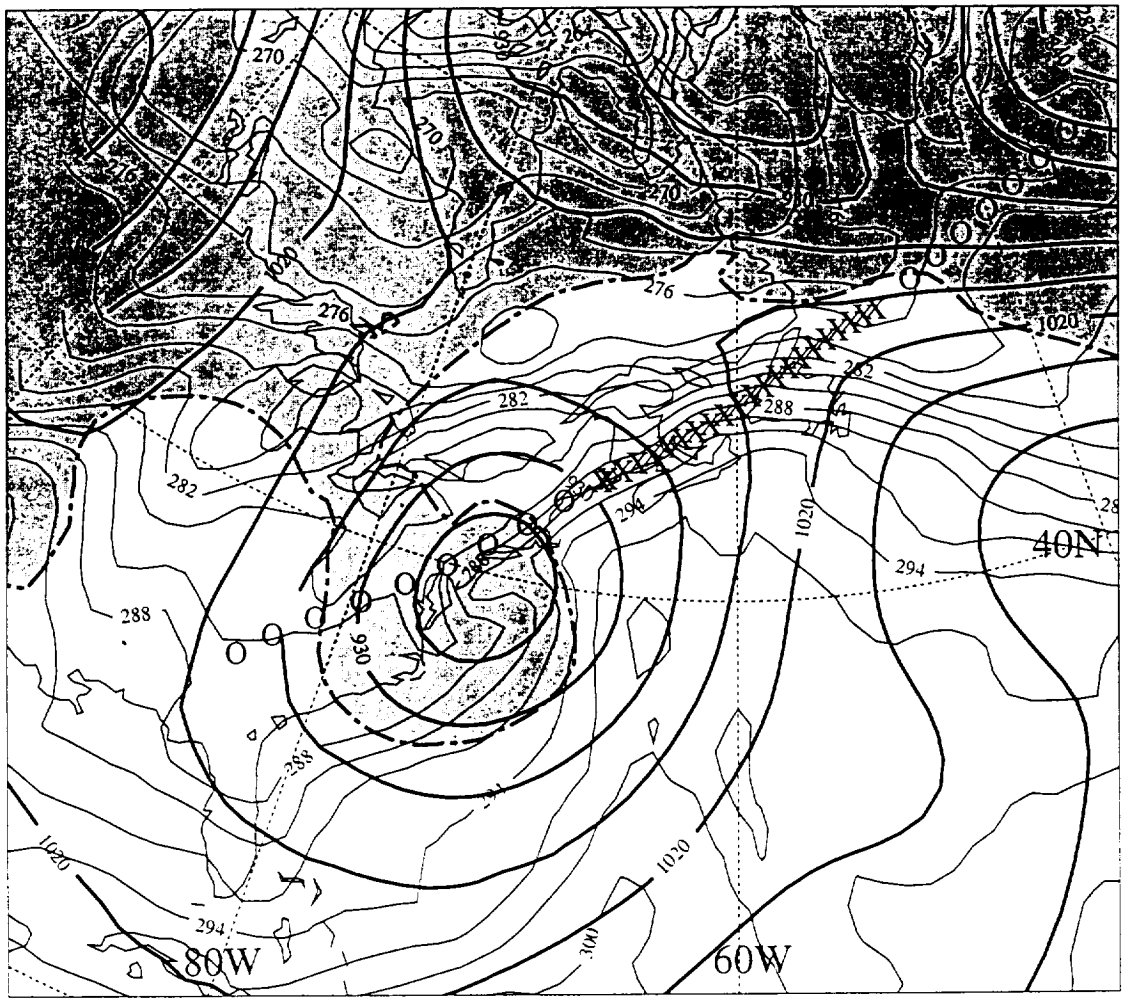
270
276
282
288
294
300
1020
930
40N
80W
60W

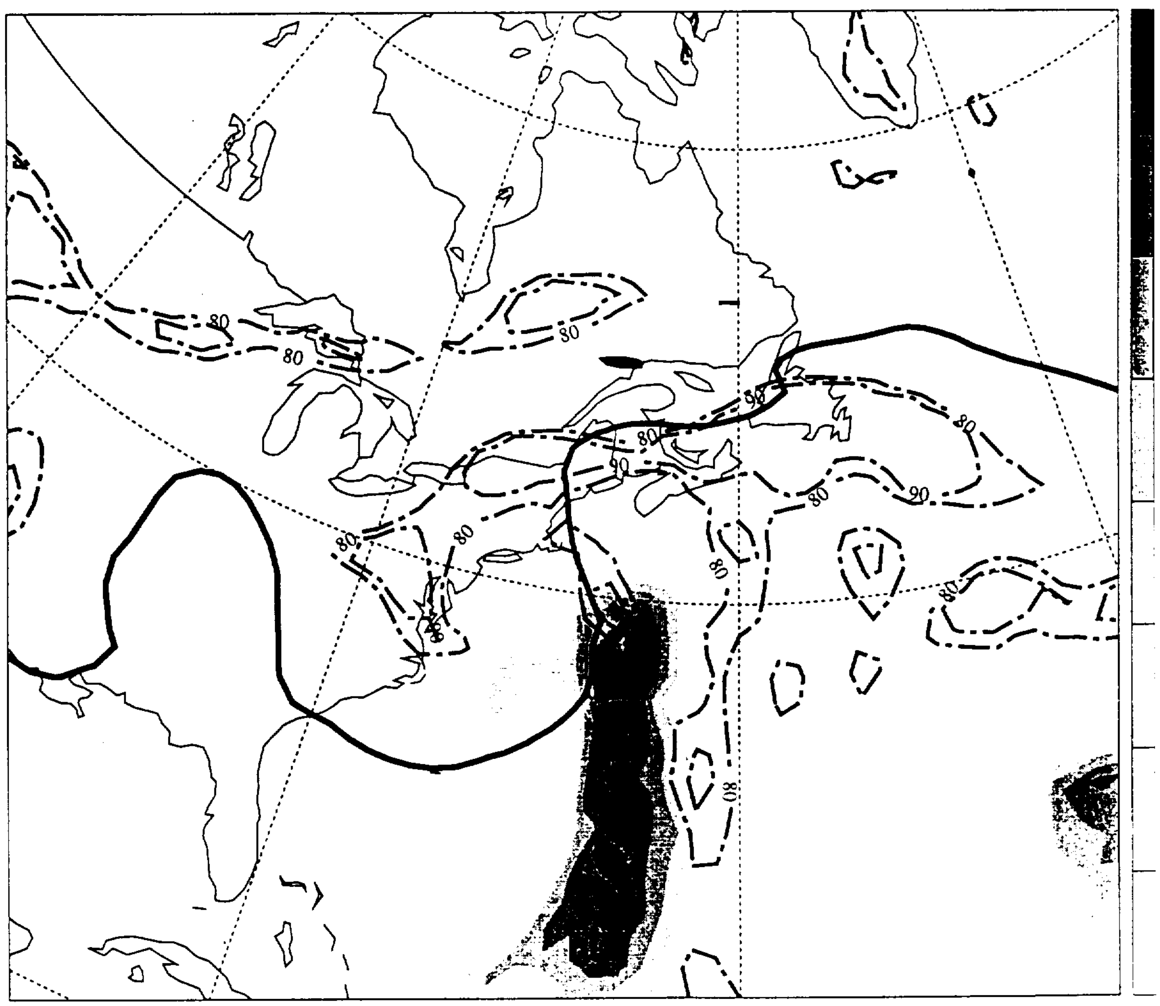
80
90

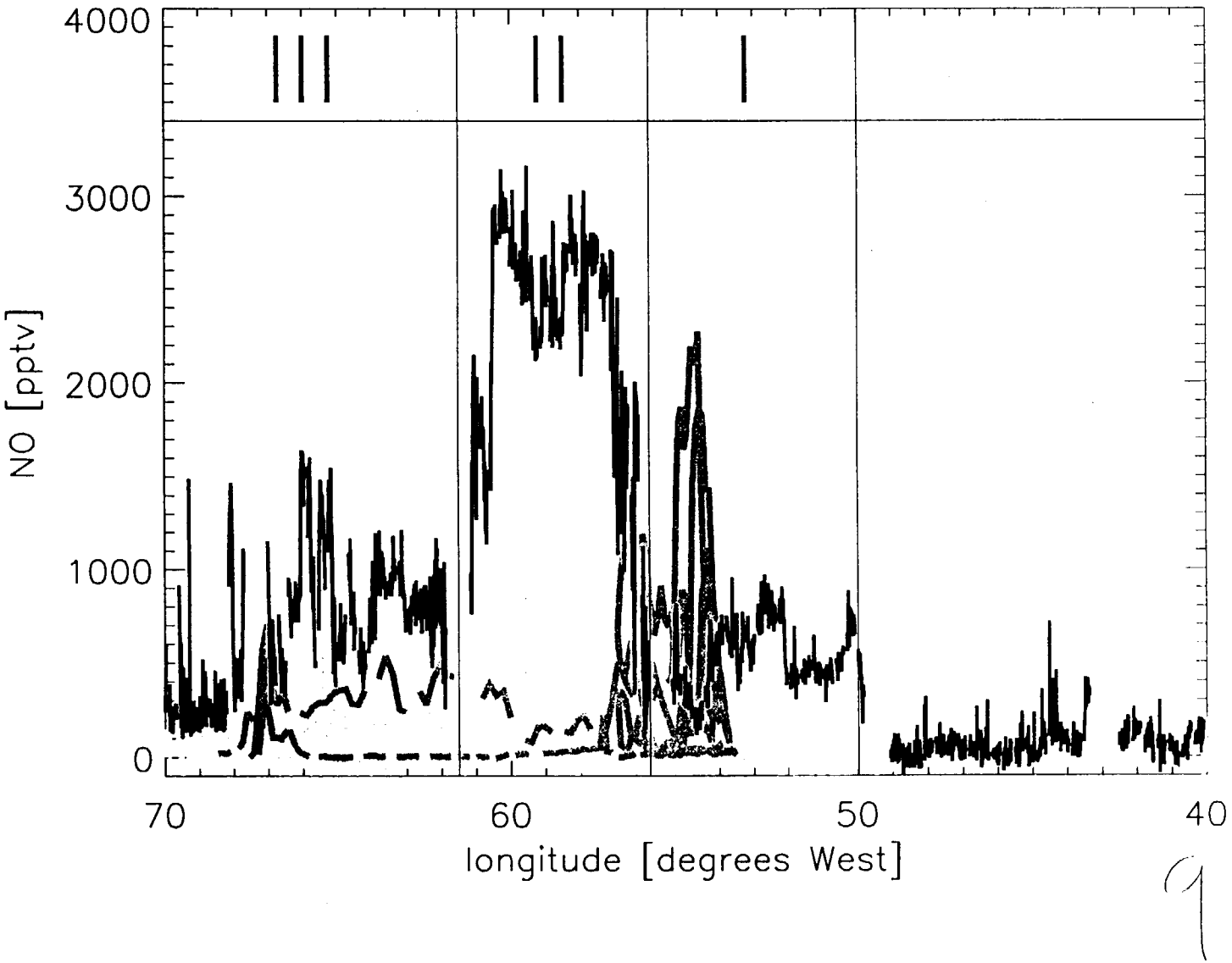
4000
3000
2000
1000
0
NO [pptv]
70
60
50
40
longitude [degrees West]

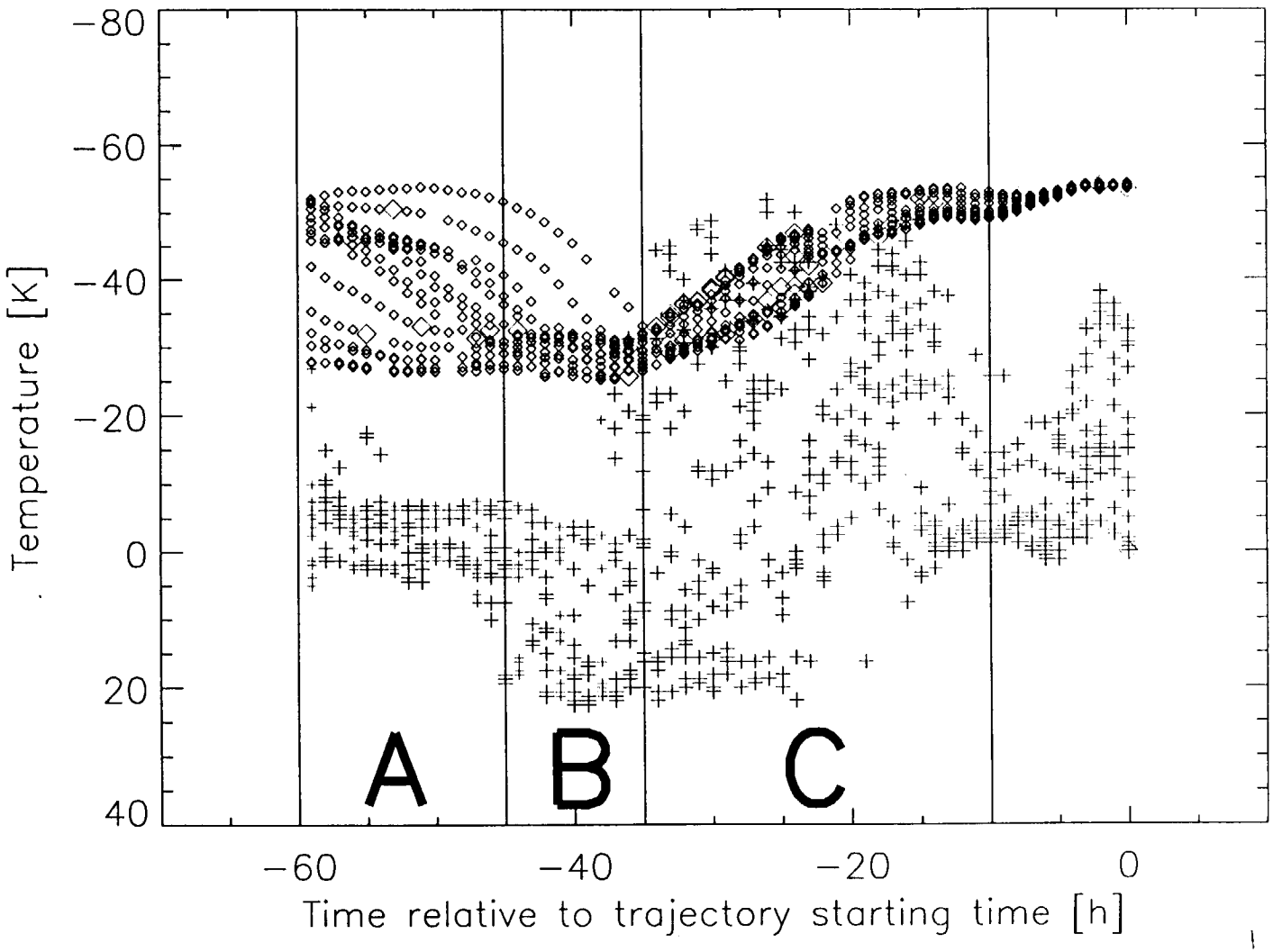
−80
−60
−40
−20
0
20
40
Temperature [K]
A
B
C
−60
−40
−20
0
Time relative to trajectory starting time [h]

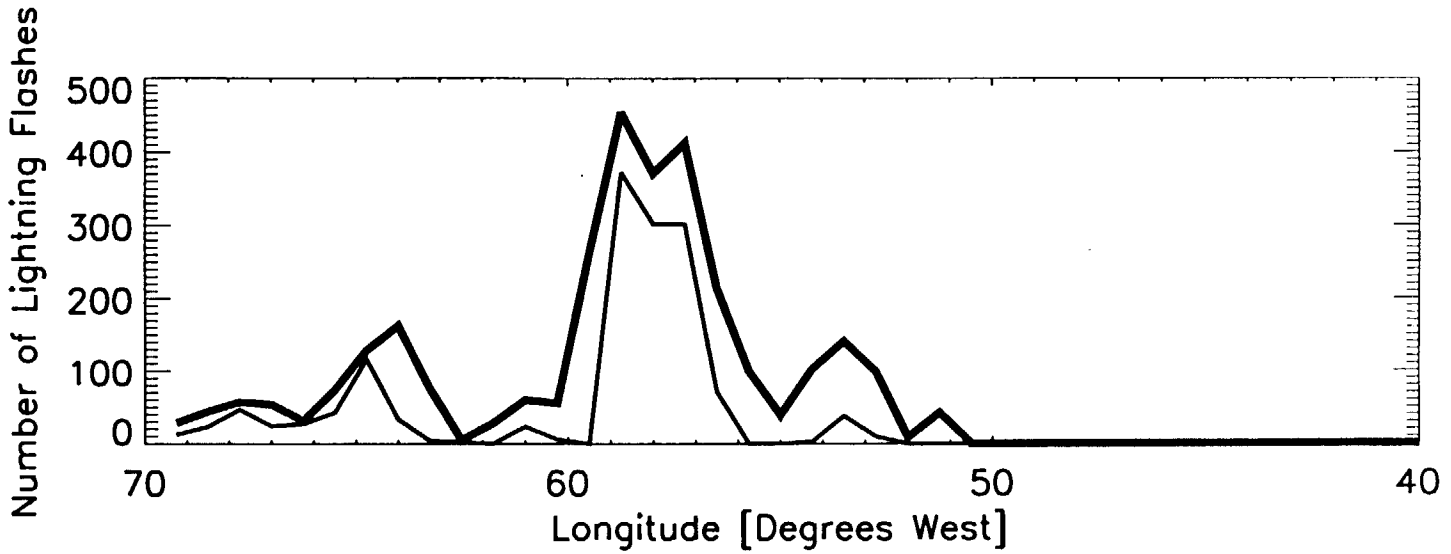
Number of Lightning Flashes
500
400
300
200
100
0
70
60
50
40
Longitude [Degrees West]

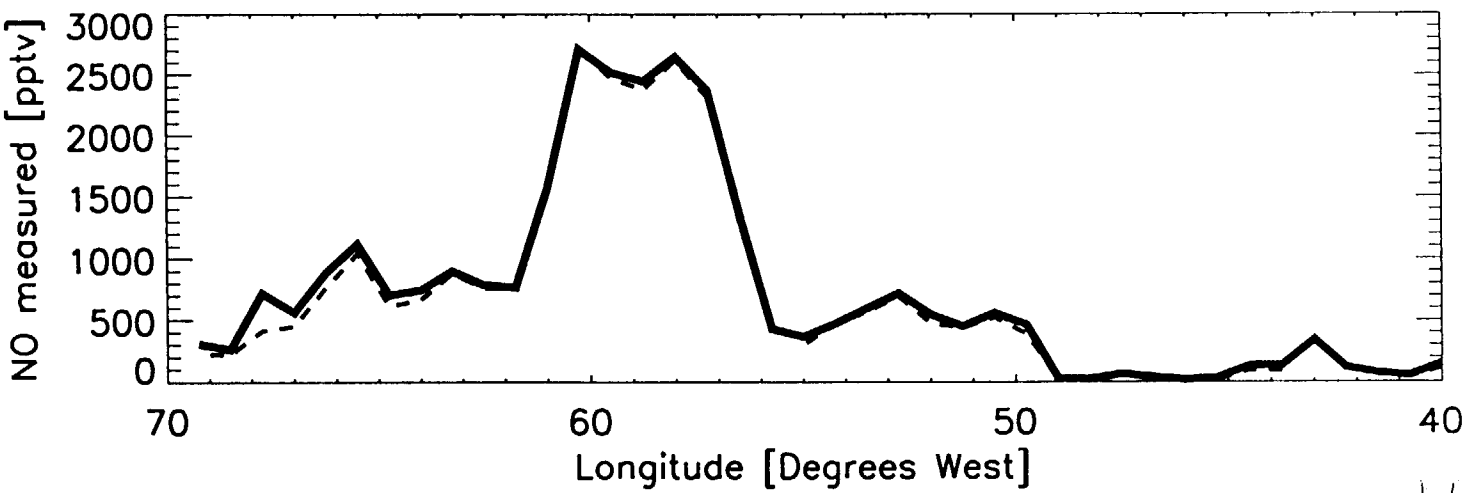
NO measured [pptv]
3000
2500
2000
1500
1000
500
0
70
60
50
40
Longitude [Degrees West]

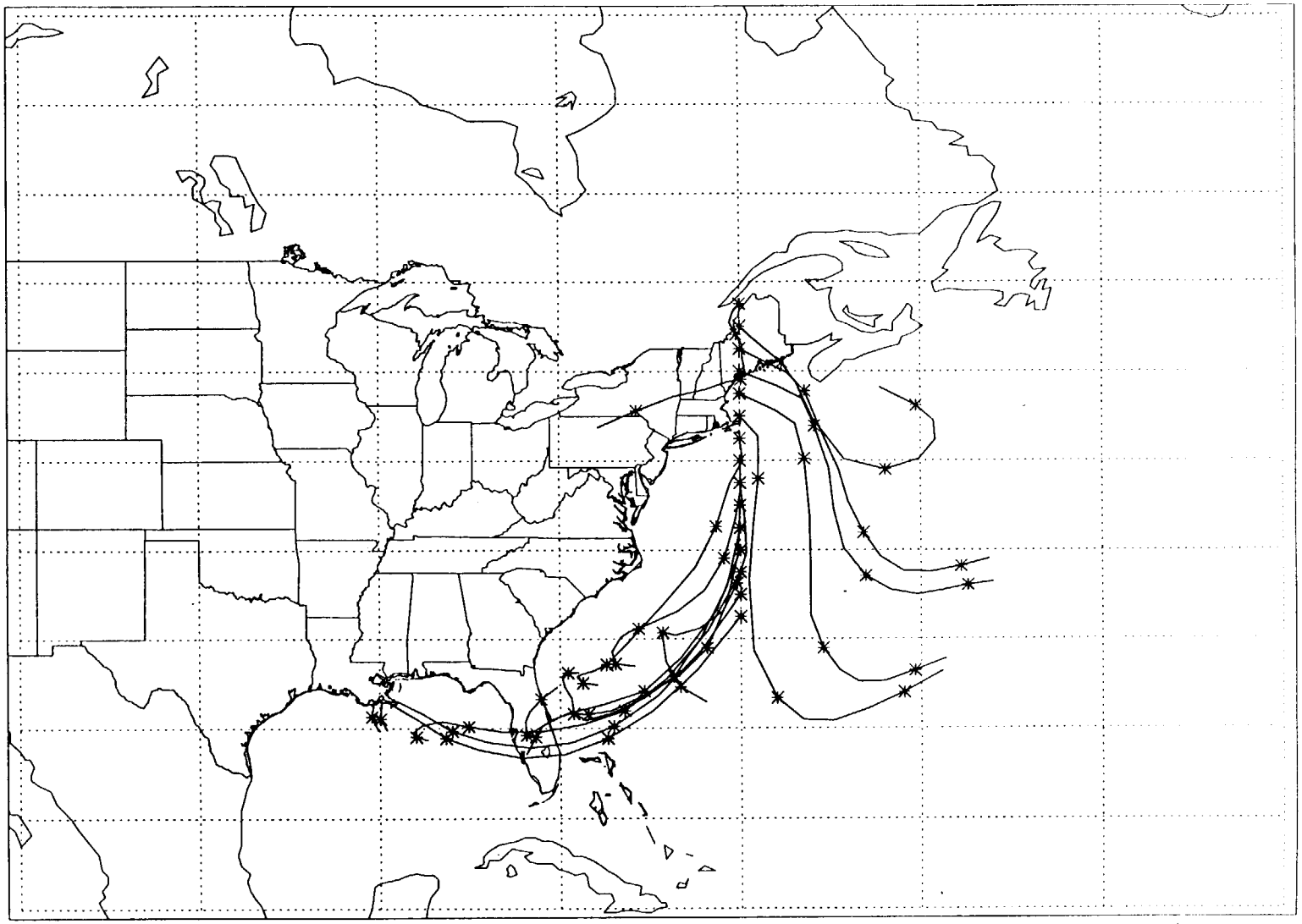

12

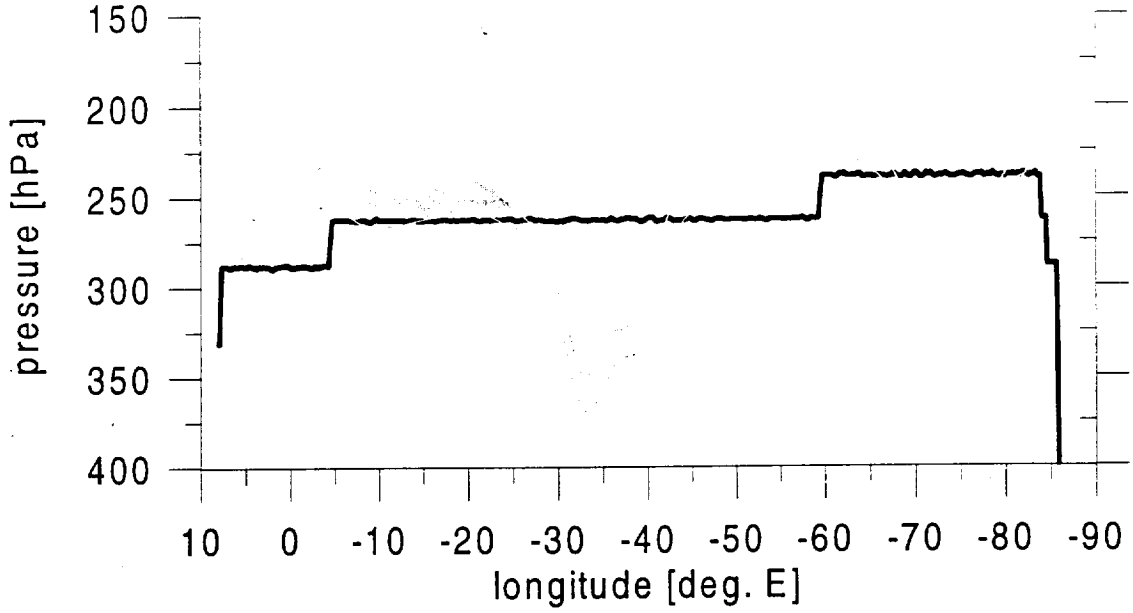
150
200
250
300
350
400
pressure [hPa]
10
0
-10
-20
-30
-40
-50
-60
-70
-80
-90
longitude [deg. E]

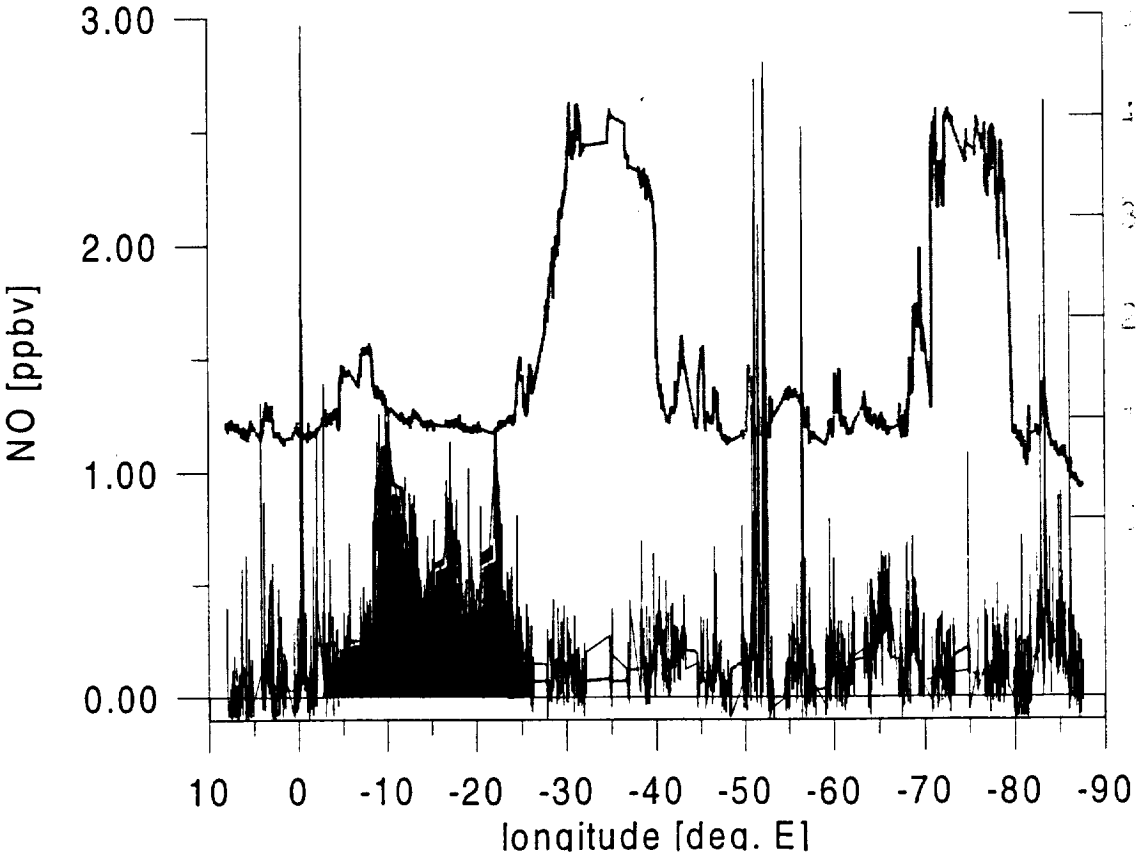
3.00
2.00
1.00
0.00
NO [ppbv]
10
0
-10
-20
-30
-40
-50
-60
-70
-80
-90
longitude [deg. E]

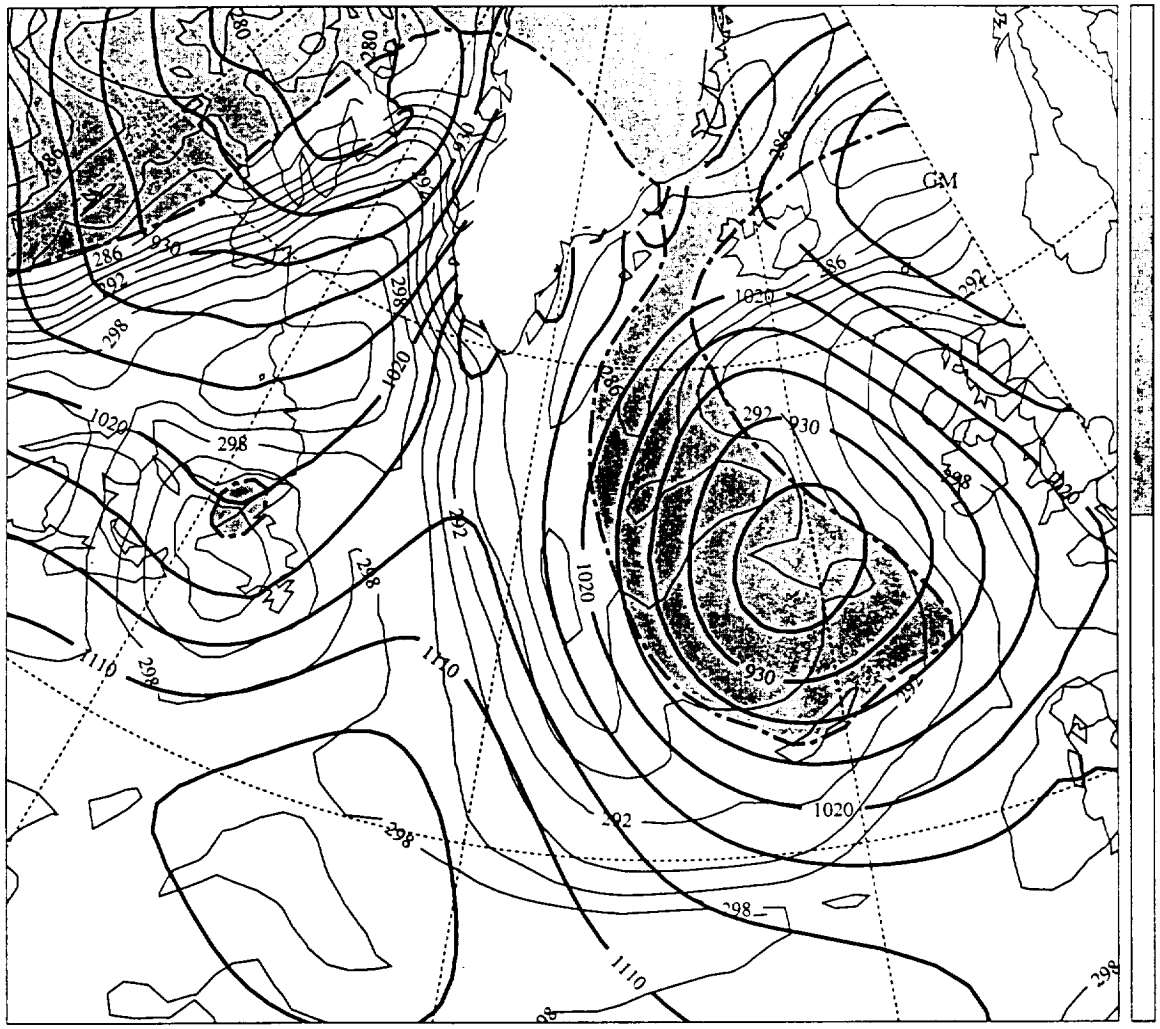

14a

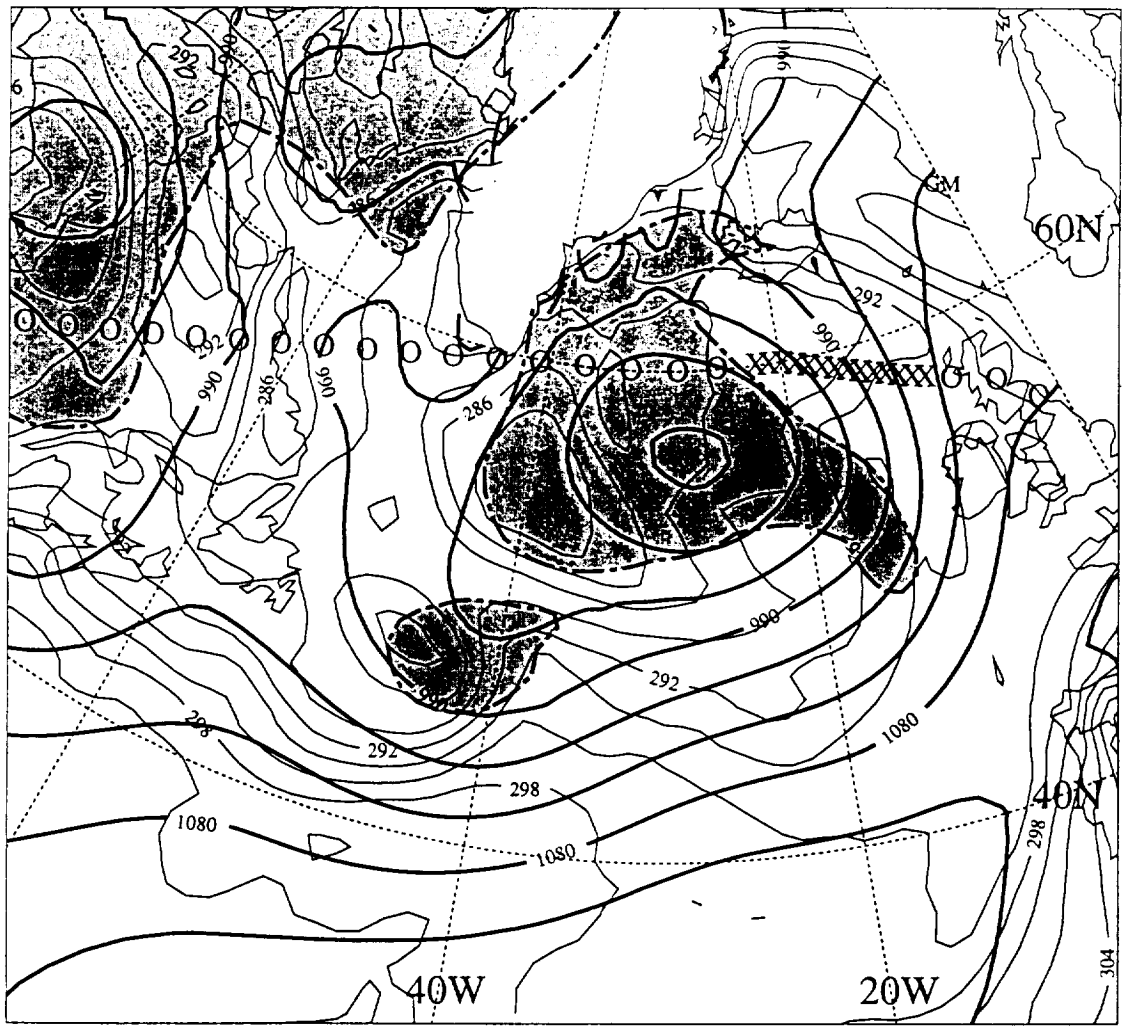
60N
40N
40W
20W
GM
292
286
990
1080
298
304

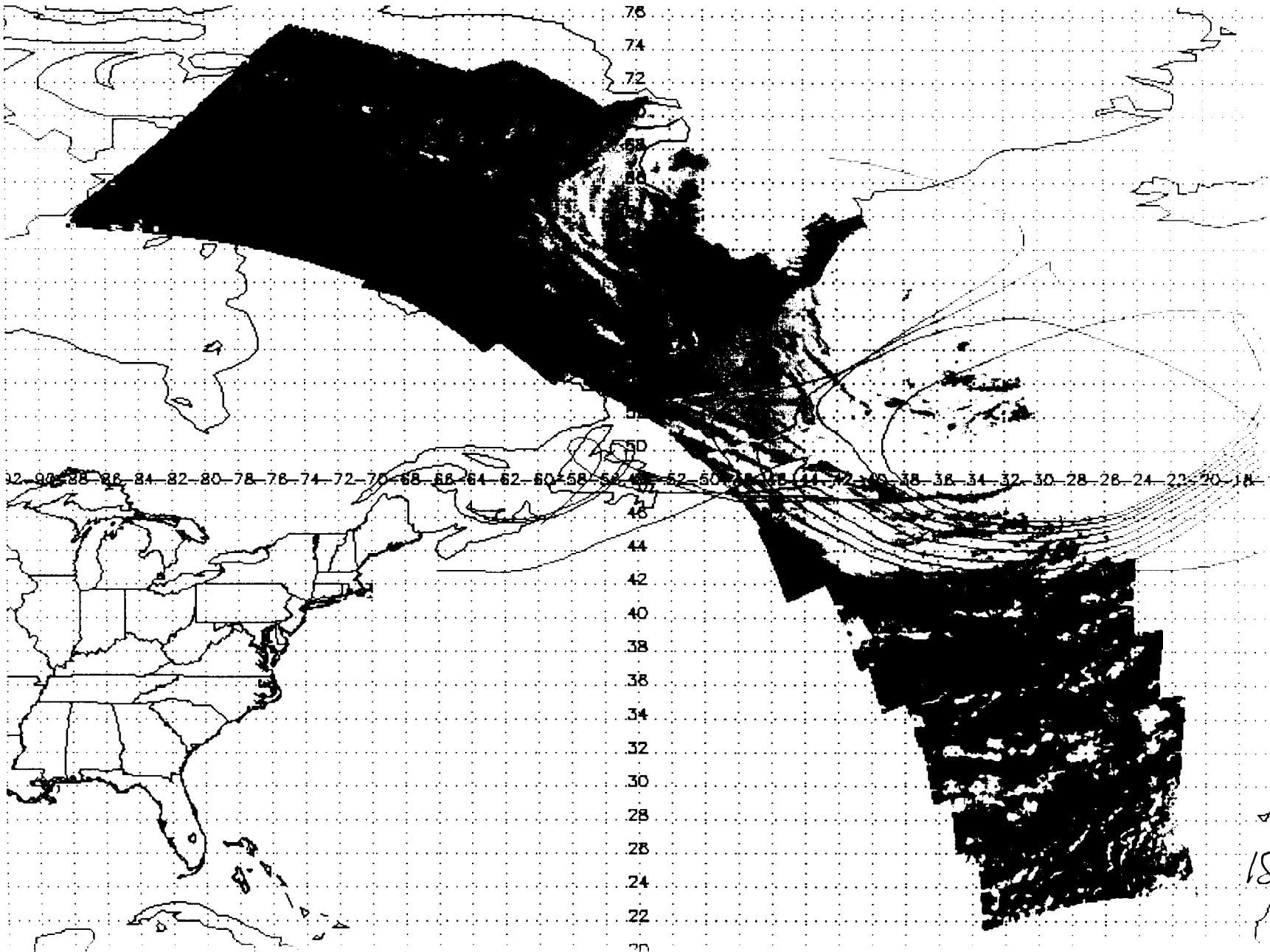

18a

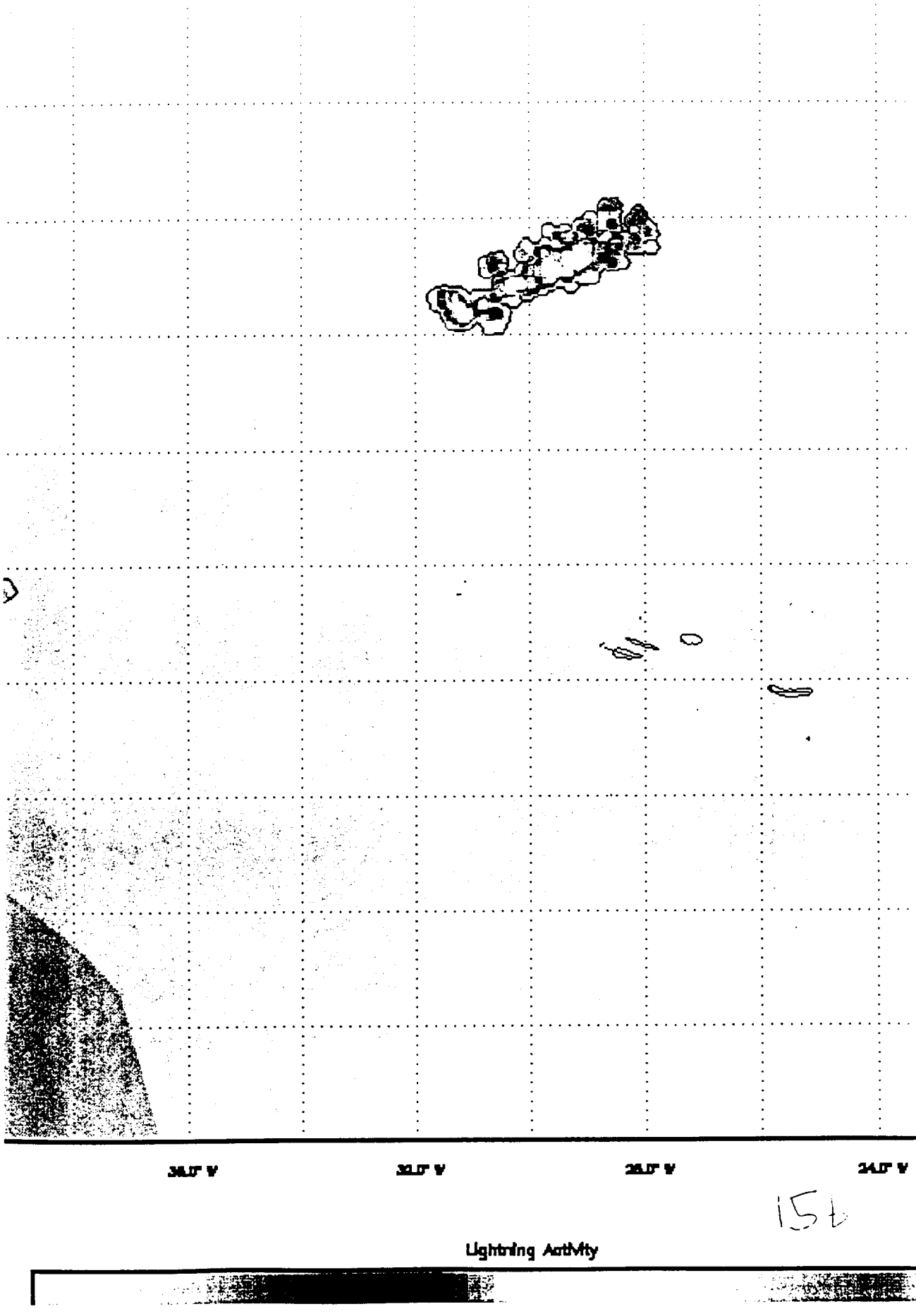
Lightning Activity

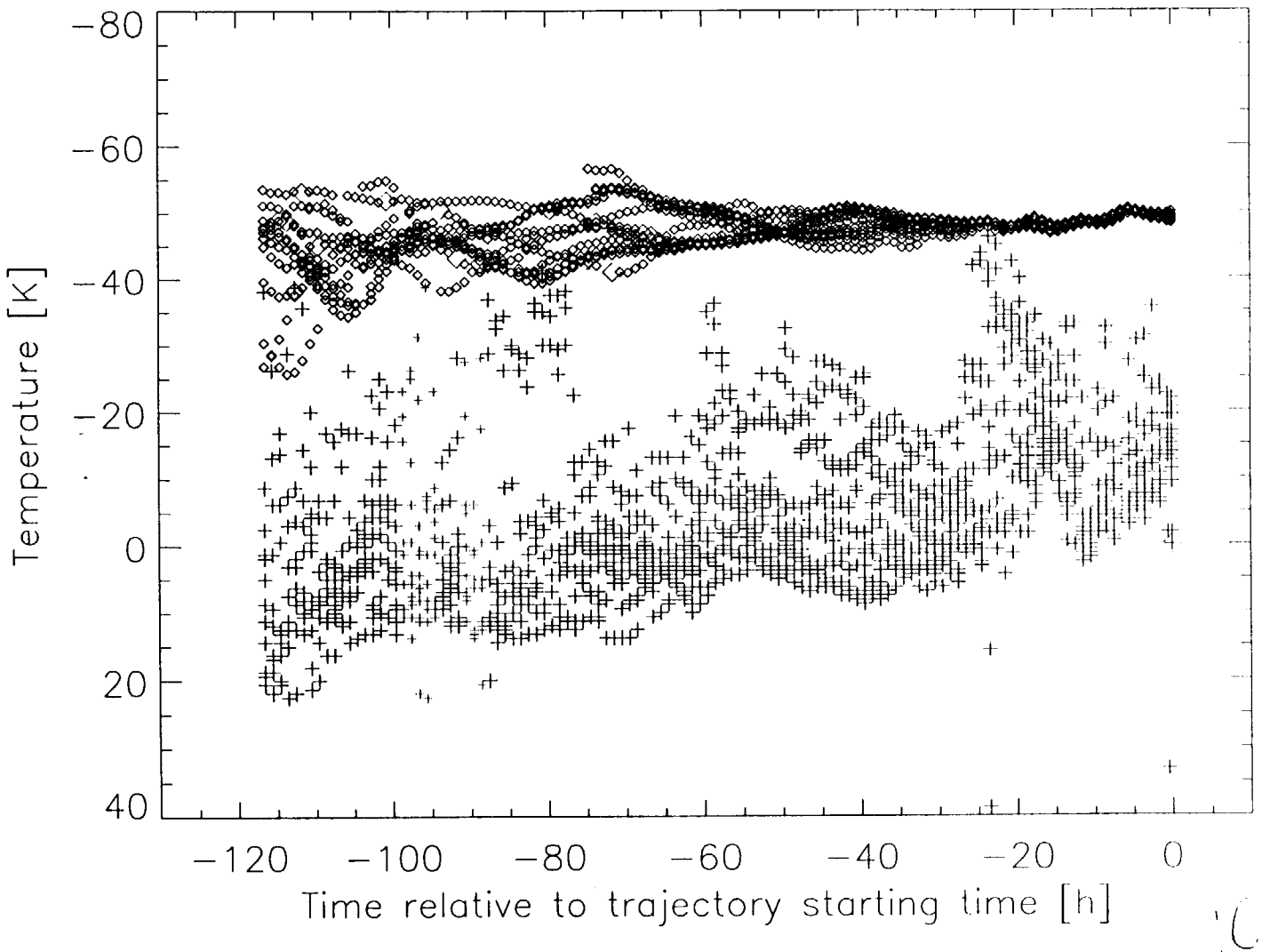
−80
−60
−40
−20
0
20
40
Temperature [K]
−120
−100
−80
−60
−40
−20
0
Time relative to trajectory starting time [h]

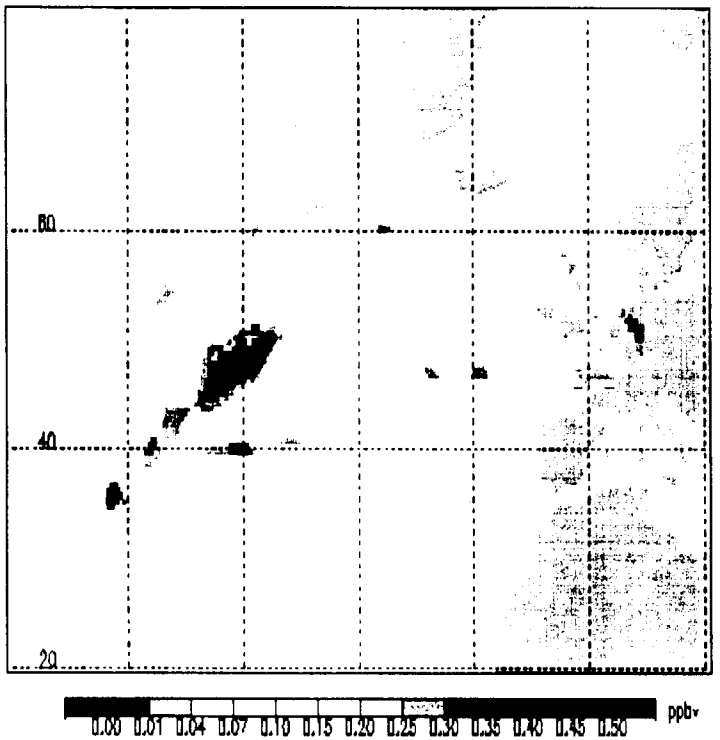
60
40
20
0.00 0.01 0.04 0.07 0.10 0.15 0.20 0.25 0.30 0.35 0.40 0.45 0.50
ppbv

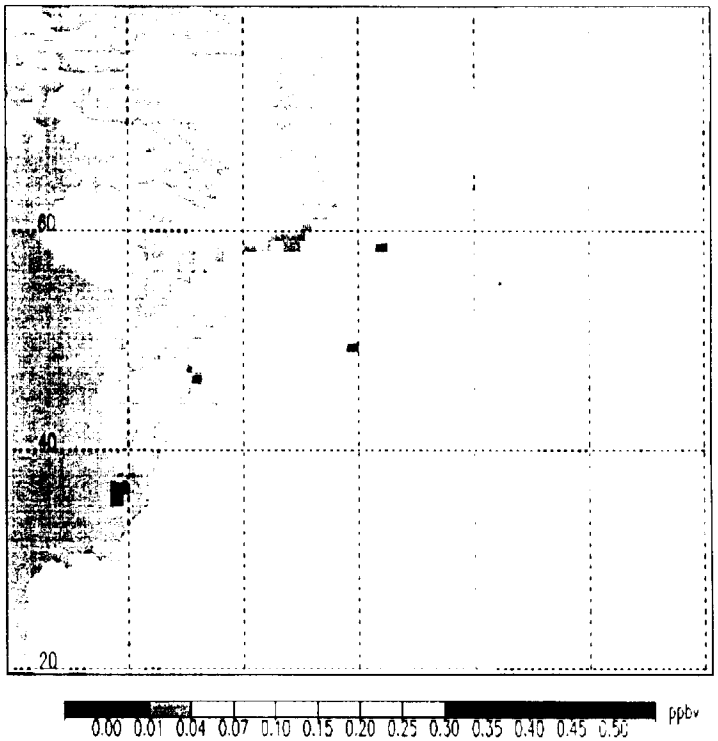
60
40
20
0.00 0.01 0.04 0.07 0.10 0.15 0.20 0.25 0.30 0.35 0.40 0.45 0.50
ppbv

17a/6

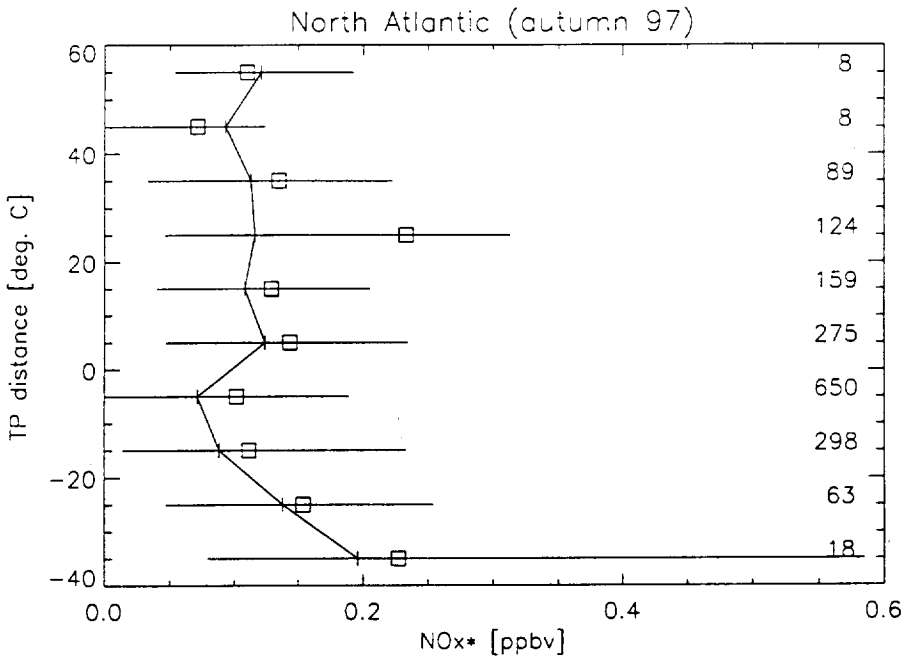
North Atlantic (autumn 97)
TP distance [deg. C]
NOx* [ppbv]
60
40
20
0
−20
−40
0.0
0.2
0.4
0.6
8
8
89
124
159
275
650
298
63
18

18a

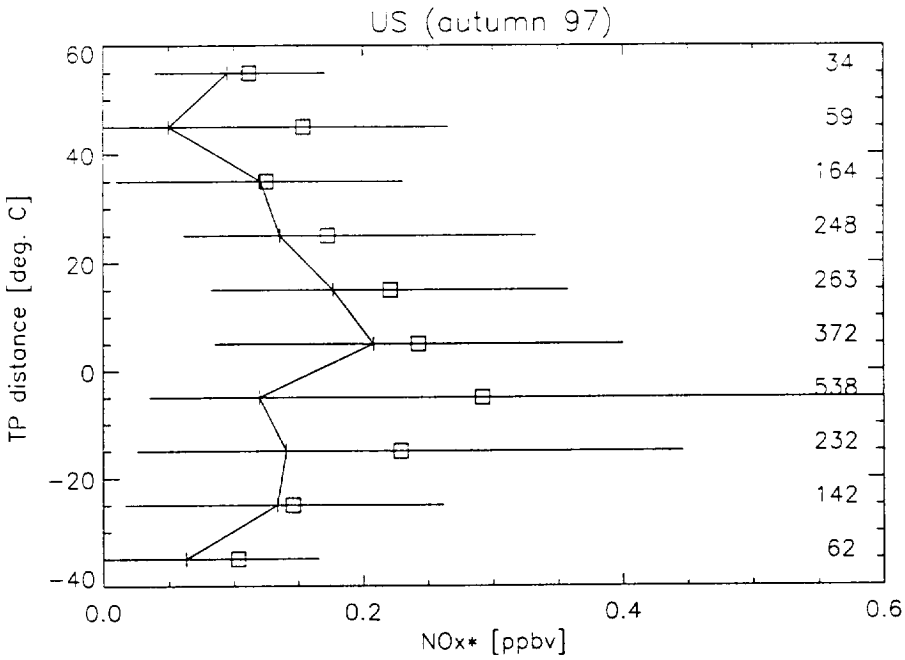
US (autumn 97)
TP distance [deg. C]
NOx* [ppbv]
60
40
20
0
-20
-40
0.0
0.2
0.4
0.6
34
59
164
248
263
372
538
232
142
62

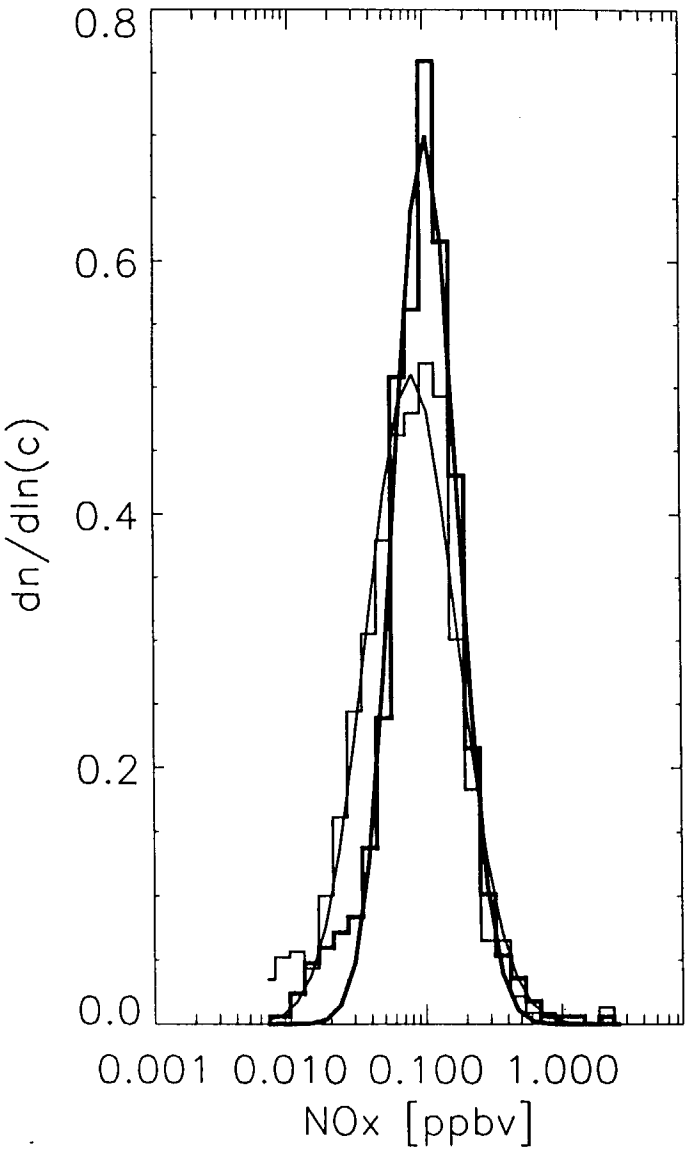
0.8
0.6
0.4
0.2
0.0
dn/dln(c)
0.001 0.010 0.100 1.000
NOx [ppbv]

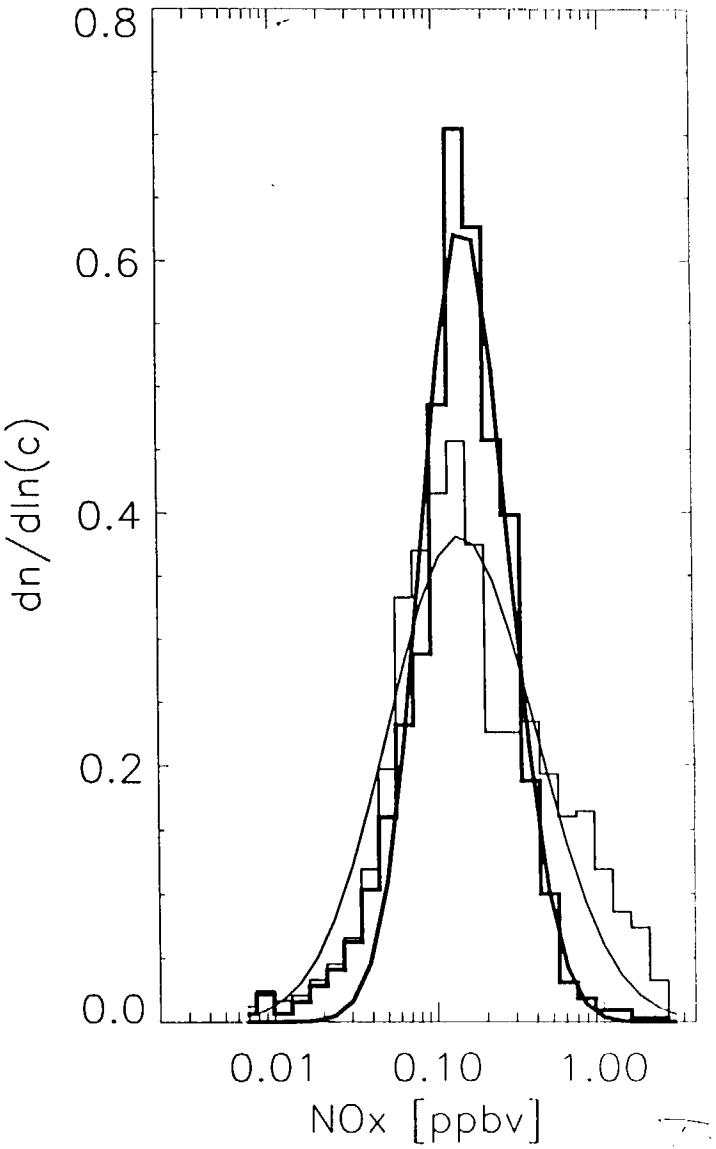
0.8
0.6
0.4
0.2
0.0
dn/dln(c)
0.01 0.10 1.00
NOx [ppbv]

Fig 18